Ecohydrology

Interplay between climate and hydrogeomorphic features and their effect on the seasonal variation of dissolved organic matter in shallow temperate lakes of the Southern Andes (Patagonia, Argentina): a field study based on optical properties

Journal:	*Ecohydrology*
Manuscript ID	ECO-16-0232.R2
Wiley - Manuscript type:	Research Article
Date Submitted by the Author:	12-May-2017

Complete List of Authors:	Soto Cárdenas, Carolina; Instituto de Investigaciones en Biodiversidad y Medioambiente (INIBIOMA, UNComahue-CONICET), Laboratorio de Fotobiología; Gerea, Marina; Instituto de Investigaciones en Biodiversidad y Medioambiente (INIBIOMA, UNComahue-CONICET), Laboratorio de Fotobiología Garcia, Patricia; Instituto de Investigaciones en Biodiversidad y Medioambiente (INIBIOMA, UNComahue-CONICET), Laboratorio de Fotobiología Pérez, Gonzalo ; Instituto de Investigaciones en Biodiversidad y Medioambiente (INIBIOMA, UNComahue-CONICET), Laboratorio de Fotobiología Diéguez, María; Instituto de Investigaciones en Biodiversidad y Medioambiente (INIBIOMA, UNComahue-CONICET), Laboratorio de Fotobiología Rapacioli, Raúl; Facultad de Ingeniería, Universidad Nacional del Comahue Reissig, Mariana; Instituto de Investigaciones en Biodiversidad y Medioambiente (INIBIOMA, UNComahue-CONICET), Laboratorio de Fotobiología Queimaliños, Claudia; Instituto de Investigaciones en Biodiversidad y Medioambiente (INIBIOMA, UNComahue-CONICET), Laboratorio de Fotobiología

Keywords:	North Andean Patagonian lakes, Seasonality, Hydrogeomorphology, Hydrological connectivity, Dissolved organic matter

Interplay between climate and hydrogeomorphic features and their effect on the seasonal variation of dissolved organic matter in shallow temperate lakes of the Southern Andes (Patagonia, Argentina): a field study based on optical properties

Carolina Soto Cárdenas,[a]* Marina Gerea,[a] Patricia E. Garcia,[a]; Gonzalo L. Pérez,[a] María C. Diéguez,[a] Raúl Rapacioli,[b] Mariana Reissig[a] and Claudia Queimaliños[a]

[a]Laboratorio de Fotobiología, Instituto de Investigaciones en Biodiversidad y Medioambiente (INIBIOMA, UNComahue-CONICET), Quintral 1250, R8400FRD, San Carlos de Bariloche, Río Negro, Argentina

[b]Facultad de Ingeniería, Universidad Nacional del Comahue, Buenos Aires1400, Q8300IBX Neuquén, Argentina

*Corresponding Author: sotocardenasc@comahue-conicet.gob.ar

Short Title:

Climate and hydrology interplay: effect on DOM properties of shallow lakes

Abstract

This study analyzes the effects of the interplay between climate seasonality and hydrogeomorphic (HGM) lake features on dissolved organic matter (DOM) properties in two neighboring shallow lakes of Andean Patagonia with different connectivity. The survey was conducted over three years at the end of the wet and dry seasons, assessing the seasonal and inter-annual variation of dissolved organic carbon (DOC) concentration, whole-lake DOC mass, and DOM quality, through chromophoric and fluorescent DOM properties (CDOM and FDOM, respectively). During the wet season (fall-winter), precipitation and runoff increased water discharge, water level and inputs of terrestrial DOM with high aromaticity, humic content and high molecular weight in both lakes. Contrastingly, during the dry season (spring-summer), in which photodegradation promoted by high irradiance and stagnant conditions drove DOM transformation, non-humic, low molecular weight DOM prevailed. Both lakes displayed synchronicity in their DOC mass, CDOM and FDOM properties, indicative of similar responses to climate forcing, although the overall impact was modulated by their HGM features. Conversely, DOC concentration showed asynchronous responses between lakes, due to the higher intensity of the dilution/evapoconcentration processes in the connected lake, highlighting that DOC concentration is not always sensitive to climate-driven forces. Overall, this study emphasizes the importance of variables other than DOC concentration, like whole-lake DOC mass, DOM quality, and HGM features, to better understand the effect of climate variability on DOM dynamics. Our results allow inferring the potential impact of an environmental scenario characterized by lower precipitation and sustained warming on DOM dynamics in Northern Andean Patagonia.

Keywords: North Andean Patagonian lakes; Seasonality; Hydrogeomorphology; Hydrological connectivity; Dissolved organic matter; Optical proxies; Allochthony; Photodegradation

1. Introduction

Climate-driven forces have profound effects on the physical, chemical, and biological properties of aquatic systems, with a stronger impact on shallow lakes due to their small volumetric buffering capacity (Adrian *et al*., 2009; Nõges, 2009; Read and Rose, 2013). The fact that shallow lakes are common and distributed worldwide (Downing *et al*., 2006; Hanson *et al*., 2007) adds value to their sentinel potential, as they capture the multiplicity of impacts induced by climate variations in different geographic and climatic regions (Adrian *et al*., 2009). In addition, shallow lakes respond rapidly to climate fluctuations, whose effects respond are reflected in variables with central roles in whole-lake functioning, such as the dissolved organic matter (DOM) pool (Reche, 2003; Williamson *et al*., 2014).

DOM is a heterogeneous mixture of substances and represents the largest pool of organic carbon (C), playing a multifaceted role in biogeochemical processes and in the metabolism of aquatic ecosystems (Wetzel, 2001). DOM increases nutrient availability, fuels microbial communities with overall cascade effects on food webs, and is an important complexing agent in natural waters, interacting with trace metals in solution (Aiken, 2014). In addition, the chromophoric fraction of DOM (CDOM) absorbs solar radiation in the ultraviolet (UV) and visible wavelengths, determining the underwater light climate (Morris *et al*., 1995) and thermal structure (Wetzel, 2001), ultimately influencing lake productivity, trophic interactions and ecosystem stability (Moran *et al*., 2000; Stedmon *et al*., 2003; Häder *et al*., 2007, 2015).

In aquatic ecosystems, DOM either derives from allochthonous sources, mostly from terrestrial vegetation and soils, or is generated by in-lake processes involving organisms (e.g., Zhang *et al*., 2009). The allochthonous inputs of DOM are positively correlated with climate-driven forces such as precipitation and surface runoff (Pace and Cole, 2002; Adrian *et al*., 2009; Garcia *et al*., 2015b). Terrestrial signals in aquatic systems are clearly expressed, particularly at moments of high connectivity with the surrounding landscape, when increased runoff delivers fresh allochthonous inputs, increasing the DOM pools of streams and lakes (Van Gaelen *et al*., 2014). Analysis of DOM through the optical properties of CDOM absorbance and its fluorescent fraction (FDOM) provides substantial information about its origin, composition, reactivity and diagenetic state, showing the degree of transformation through photochemical and/or biological processing (Del Vecchio and Blough, 2004; Kowalczuk *et al*., 2009; Zhang *et al*., 2009).

Several studies have highlighted the modulating role of hydrogeomorphic (HGM) features of aquatic systems in their linkage with the surrounding landscape (Webster *et al*., 2008; Queimaliños *et al*., 2012; Köhler *et al*., 2013; Weyhenmeyer *et al*., 2016). For instance, the water residence time (WRT) affects DOM processing by controlling exposure to photochemical and biological transformation (Bertilsson and Tranvik, 2000; Guillemette and del Giorgio, 2011), as well as DOM loss through mobilization to the sediments and respiration (von Wachenfeldt *et al*., 2008; Kothawala *et al*., 2014). The lake morphometry affects thermal resilience and evaporative exchange, driving the photochemical transformation of DOM (Reche *et al*., 2000; Williamson *et al*., 2014).

Several short- and long-term studies on DOM dynamics in lakes of the Northern Hemisphere have shown a dramatic increase in their dissolved organic carbon (DOC) concentration (Roulet and Moore, 2006; Monteith *et al*., 2007; Weyhenmeyer *et al*., 2016). There is now convincing evidence that the magnitude and regulation of the increase in aquatic DOC (browning) is mostly driven by climate trends that promote terrestrial exports, including rising temperatures, CO_2 enrichment and recovery from acidification (Evans *et al*., 2006; Erlandsson *et al*., 2008; Weyhenmeyer and Karlsson, 2009; Larsen *et al*., 2011; Weyhenmeyer *et al*., 2016).

The temperate regions of South America are also showing the impact of a changing climate (IPCC, 2013; Barros *et al*., 2015). In particular, the southern region of South America and Patagonia is undergoing significant and extensive hydroclimatic fluctuations (Masiokas *et al*., 2008). During the last four decades, the westerly flow over northern central Patagonia has decreased, causing a drying trend to the west of the Andes, and there is also a pattern of subtle but widespread warming in the region (Garreaud *et al*., 2013). If sustained over time, these changes will probably influence allochthonous inputs to aquatic systems, thereby influencing DOM concentration and its in-lake processing. The lakes of the Andean Patagonian region hold great potential as sentinels of climate change, due to the fact that they are pristine oligotrophic systems with none to low human impact, subject to a sustained regional decrease in precipitation and rising temperatures. In contrast, the temperate lakes of the Northern Hemisphere exhibit the impact of complex interactions between climate change and anthropogenic stressors, which hinder the interpretation of climatic signals (Evans *et al*., 2006).

Within the extended Patagonian region (39° to 55° S), the northernmost area presents marked seasonality in the precipitation regime, with well-defined wet (fall-winter) and dry (spring-summer) seasons (Paruelo *et al*., 1998; Bianchi *et al*., 2016). Furthermore, this region experiences high solar radiation levels, especially UV, from the beginning of the dry season, which promotes photo-induced chemical and biological DOM processing (Zagarese *et al*., 1998). The strong contrasting seasonal patterns of precipitation and solar radiation exposure acting on temperate lakes of northern Patagonia are amenable to analysis of the impact of terrestrial DOM inputs and photodegradation processes as drivers of lake DOM. In fact, it has been found that shallow lakes of northern Patagonia show a positive relationship between precipitation and CDOM properties (i.e, molecular weight and water color) (Gerea *et al*., 2016).

Similar ecosystem properties have commonly been observed in lakes exposed to the same climatic temporal variations. Indeed, in lakes located inside small geographic districts (<100

Km), climatic forcing regulates seasonal and inter-annual synchrony among physical and chemical lake variables (Pace and Cole, 2002; Vogt *et al*., 2011). However, water bodies on a small spatial scale could provide further insights into the interaction between catchment and climate features and its effect on DOM quality (Massicotte and Frenette, 2011; Kothawala *et al*., 2014). The objective of the current study was to analyze the interplay between climate seasonality and HGM lake features, and determine how they affect DOM concentration and quality in two shallow neighboring lakes of North Patagonia with different connectivity. We selected a hydrological network on a restricted spatial scale, featuring one lake located in a chained lacustrine system and another one located in a closed basin (Lake Morenito and Lake Escondido, respectively) (Lirio, 2011; Gerea *et al*., 2016). We performed a synchronous comparative study of the DOM pools, characterized through CDOM and FDOM analyses, which provide complementary information on the DOM source, quality and processing. We hypothesized that under the same climatic conditions, the contrasting HGM and hydrological connectivity of the lakes will be reflected in different DOM properties. The study was conducted over three consecutive years, with sampling scheduled at the end of the wet season to capture the input of terrestrial DOM and at the end of the dry season to assess in-lake processing. Thus, both temporal and spatial scales were considered. The temporal variability within each lake was assessed seasonally and inter-annually (within-lake variability), while the spatial scale was used to compare responses between lakes (between-lake variability).

2. Material and Methods

2.1. Study site

Lakes Morenito and Escondido belong to the Nahuel Huapi catchment (Nahuel Huapi National Park, Andean North Patagonia, Argentina), located inside the Glacial Lake District (Iriondo, 1989; Figure 1). These lakes are situated in an elevated piedmont area (~800 m a.s.l.) and are surrounded by a perennial temperate forest. Lake Morenito (41°03'S, 71°34'W, 768 m a.s.l., Z_{max}=10.5 m) is part of an open basin, connected upstream with Lake Ezquerra (Z_{max}=4 m; Pérez *et al*., 2010) and downstream with Lake Moreno West (Z_{max}=90 m; Queimaliños *et al*., 2012). Lake Morenito was an open bay of Lake Moreno West until 1960, when the construction of a gravel road separated the systems, limiting their connectivity to a channel. In addition, Lake Moreno West is connected through a short narrow stream (0.5 km) with Lake Nahuel Huapi, the largest lake (surface=557 km^2; Z_{max}=464 m) of the North Andean Patagonian sector at the eastern side of the Andes (Figure 1). In this chained lacustrine system, water flows from Lake Ezquerra to Lake Morenito and then to Lake Moreno West (Figure 1). Long-term lake water storage datasets indicate a maximum variation in the water level of Lake Nahuel Huapi of 3.2 m, with the lowest level occurring during summer (December to March), followed by an increase from April (southern fall), and reaching the highest level between July and November (*Autoridad Interjurisdiccional de Cuencas*, AIC, 2015) (Figure 1). Lakes Moreno West and Morenito also display this seasonal change in their water levels due to their connection with Lake Nahuel Huapi (Rapacioli, 2011). In contrast, Lake Escondido (41°03'S, 71°34'W, 770 m a.s.l., Z_{max}=8.3 m) is located 3 km west of Lake Morenito, in a small closed basin lacking major streams (Lirio, 2011), and receives inputs from small temporary water courses during rainy periods. Although this lake is adjacent to Lake Nahuel Huapi (Figure 1), a separation of 3 m in height prevents their direct connection (Lirio, 2011).

Lakes Morenito and Escondido are cold and polymictic, freezing occasionally during strong winter periods and eventually stratifying during late spring or early summer (Queimaliños, 2002; Bastidas Navarro *et al*., 2009). Both lakes are oligotrophic, their water columns are illuminated down to the bottom (Gerea *et al.*, 2016), and they have similar aquatic vegetation characterized by the occurrence of emergent stands of *Schoenoplectus californicus* in littoral sectors and spots of *Potamogeton linguatus*.

The Andean region of North Patagonia is characterized by a transitional oceanic-continental cold climate with a dry summer (Köppen *Csb*), governed by the prevailing westerly winds coming from the South Pacific subtropical anticyclone. The wet season coincides with the cold period (April to September) and concentrates 73% of the annual precipitation (mean annual precipitation ~1800 mm y^{-1}) (Paruelo *et al*., 1998; Rapacioli, 2011), while the dry season (October to March) coincides with the maximum incidence of solar radiation (Díaz *et al*., 1994). These features determine two contrasting scenarios: a cold winter period, characterized by low irradiance, low air temperature and high precipitation and runoff, and a warm period, characterized by high irradiance, moderate to high air temperature and dry conditions (Paruelo *et al*., 1998; Soto Cárdenas, 2015).

2.2. Precipitation, temperature and solar radiation patterns

The precipitation data of the period studied (2012–2015) were recorded at a meteorological station (AIC) located ~1.1 km from Lake Escondido and ~3.8 km from Lake Morenito. The monthly cumulative precipitation was calculated to describe the annual precipitation pattern. To explore the effect of cumulative precipitation on the seasonal trend of CDOM, linear regression analysis was applied using different time intervals (of 30 days) for the cumulative precipitation before sampling (30 to 360 days). The cumulative precipitation of the 150 days previous to the sampling (0-150 days) was the best explanatory variable of the natural precipitation pattern, as reported previously by Gerea *et al*. (2016), and was thus included in the analyses.

Air temperature and photosynthetically active radiation (PAR) at ground level were obtained from the monitoring station EMMA (Photobiology Laboratory, INIBIOMA, Bariloche, Río

Negro, Argentina) located 10 km east of the sampling sites. PAR irradiance (μmol cm^{-2} s^{-1}) was measured with a band radiometer GUV 511 (Biospherical Instruments, Inc.). Daily fluence (μmol m^{-2}) was calculated as irradiance converted to m^2 and multiplied by 86400 s (=24*60*60). Monthly fluence (mmol m^{-2}) was then calculated from the daily fluence data. Also, the fluence of the 150 days previous to the sampling (fluence 150d) was estimated to evaluate its cumulative effect in dry and wet periods. These cumulative values were used in the multivariate statistical analysis (RDA) (see below).

2.3. Calculation of HGM features and catchment areas

Bathymetric maps depicting the high water phase of lakes were used to calculate HGM features such as area, perimeter, volume (V), and maximum and mean depth (Z_{max} and Z_{mean}) during the wet season. Lake volume was calculated by integrating the area delimited by the hypsographic depth-area curves (Wetzel, 2001). Areas (A) and perimeters (P) of the lakes during the dry season were calculated from Google Earth® maps portraying the low water phase (Figure 1C,D). These data, together with the seasonal water level variation, were used to calculate lake volume in the low water phase. Variations in the water level were recorded on each sampling occasion from hydrometric rods placed on the shore of each lake. The perimeter:area ratio (P:A) was calculated to explore the areal terrestrial carbon loading to the lakes (Webster *et al.*, 2008).

The catchment or drainage areas (D) and the ratio of drainage area to lake area (D:A) were calculated by applying Digital Terrain Models based on maps published by ASTER-GDEM[1]. In the case of Lake Morenito, the drainage area was calculated including the upstream Lake Ezquerra. Forested and urban areas within lake catchments were estimated from Rapacioli (2011). The percentage of water in the surrounding catchment (%Water) was calculated as the relative areal coverage of open water in the catchment not including the lake itself (Kothawala *et al.*, 2014; Kellerman *et al.*, 2014). The mean annual water discharge of each lake [Q_{mv} (L s^{-1})] was calculated using precipitation data, evaporation volumes and runoff inputs obtained through hydrometeorological processed data. Water retention times (WRT) were estimated as mean lake Volume/annual Q_{mv} (Håkanson, 2005). Finally, seasonal precipitation, evaporation volumes, and runoff inputs were used to calculate the mean water discharge in the wet and dry seasons (seasonal Q_{mv}).

2.4. Sample collection and processing

[1] The Advanced Space borne Thermal Emission and Reflection Radiometer (ASTER) Global Digital Elevation Model (GDEM) was developed jointly by the Japanese Ministry of Economy, Trade, and Industry (METI) and the United States National Aeronautics and Space Administration (NASA).

Lakes Morenito and Escondido were sampled at the end of the dry and wet seasons over three consecutive years (2013 to 2015). In Lake Escondido, the sampling was performed on five dates (except in the wet season of 2015). This seasonal sampling schedule was based on a previous study (Gerea *et al*., 2016), which helped us to identify the end of the dry and wet seasons as key moments for DOM analysis in these lakes. Due to the small size of both lakes, the water sampling was carried out in one station located in the deepest part of each lake and at four different depths (0, 3, 6 and 7 or 8 m) depending on the water level. Samples were taken with a Kemmerer bottle, poured into 5 L acid-washed and pre-rinsed polypropylene containers, and transported insulated to the laboratory within 1 h of sampling. Temperature, pH and conductivity were recorded on each sampling occasion.

2.5. Laboratory analyses

A volume of 1-3 L from each water sample was filtered through pre-combusted glass fiber filters (GF/F Whatman) to assess chlorophyll *a* (Chl*a*) concentration by extraction with 90% ethanol, followed by absorbance measurements after Nusch (1980).

Pre-filtered (0.7 µm GF/F), sterile (0.22 µm PVDF Millipore) water samples were used to determine DOC concentration and characterize DOM. DOC concentration was measured with a Shimadzu TOC-L analyzer (Shimadzu Corporation, Japan). DOM was characterized through UV-visible and fluorescence spectroscopy. The UV-visible absorbance spectra were obtained using a spectrophotometer (Shimadzu UV-1800) in a 10cm quartz cuvette, recording absorbance values between 200 and 800 nm, at 1 nm intervals. Milli-Q water was used as blank. Average absorbance from 700 to 800 nm was subtracted from each spectrum to correct for offsets due to several instrument baseline effects (Helms *et al*., 2008). Absorbance units were converted to absorption coefficients as follows:

$a = 2.303\ A/l$

where,

a= Naperian absorption coefficient (m^{-1}),

A= absorbance

l = path length (m).

CDOM absorption was characterized at three reference wavelengths: two in the UV spectral region (254 and 350 nm) (Reche *et al*., 1999; Spencer *et al*., 2009) and the other in the visible region (440 nm) as a proxy for water color (Reche *et al*., 1999). The absorption coefficients a_{254} and a_{350} nm normalized by the DOC concentration (a_{254}:DOC or $SUVA_{254}$ and a_{350}:DOC) were used as surrogates for DOM aromaticity (Weishaar *et al*., 2003) and lignin content, a tracer of terrigenous DOC (Fichot and Benner, 2012), respectively. Both coefficients were expressed as L mg^{-1} m^{-1}. The spectral slope for the 275-295 nm interval ($S_{275\text{-}295}$; 10^{-3} nm^{-1}) was calculated by fitting a linear regression to the log-transformed spectra, as described by Helms *et al*. (2008). $S_{275\text{-}295}$ is inversely related to DOM molecular size and is thus widely used as a proxy for photochemical degradation (Helms *et al*., 2008; Fichot and Benner, 2012).

The whole-lake DOC mass (expressed as tons of C) for the dry and wet seasons for each lake was determined by multiplying lake volume by the corresponding DOC concentration value.

FDOM was characterized with a Perkin-Elmer 55B spectrofluorometer equipped with a 150-W Xenon arc lamp and a Peltier temperature controller, using a 1 cm quartz fluorescence cell. Excitation-emission matrices (EEMs) were obtained at excitation wavelengths from 240 to 450 nm, every 5 nm, slit width 15 nm and emission wavelengths from 300 to 598.5 nm every 0.5 nm, slit width 15 nm at a scan speed of 1500 nm min^{-1} (integration time of 0.2 sec). Milli-Q blanks were measured daily. The EEMs were processed with the FL–WinLab software. Absorbance was measured concurrently using a UV-visible spectrophotometer to correct measurements for the inner filter effect. The EEMs were corrected using the toolbox FDOMcorr for MATLAB (MATLAB®R2015b, The Natick, USA) for instrument bias and inner filter effect, subtracting the water blank and normalizing to the area under Raman peaks of the blank (λ_{Ex}= 350 nm), expressing the data in Raman Units (R.U.), following Murphy *et al.* (2010).

In addition, fluorescence-based indices were calculated to assess the FDOM features. The humification index (HIX) (Zsolnay *et al*., 1999; modified by Ohno, 2002) and the biological index (BIX) (Huguet *et al*., 2009) were calculated to assess the degree of humification and autotrophic production of FDOM, respectively. HIX was determined from the ratio of two integrated regions of an emission scan [$Em_{435–480}$: ($Em_{300–345}$+ $Em_{435–480}$)] collected at an excitation of 254 nm (Ex_{254}). This index ranges from 0 to 1, with higher values indicating a greater degree of humification (Ohno, 2002). BIX was obtained as the ratio of the emission intensities at 380 and 430 nm (Em_{380} and Em_{430}), using a fixed excitation at 310 nm (Ex_{310}). This index is influenced by the presence of two common peaks in the fluorescence spectra, which have been attributed to terrestrial and microbial components. High values of BIX (>1) correspond to a predominantly autochthonous origin of DOM, whereas lower values of BIX (0.6–0.7) indicate a comparatively lower production of autochthonous DOM (Huguet *et al*., 2009). The fluorescence index (FI) was calculated as the ratio of the emission intensities at 450 and 500 nm, with an excitation at 370 nm. This index was applied to differentiate precursor DOM sources (i.e., aquatic vs. terrestrial), ranging from 1.4 to 1.5 for terrestrial DOM and from 1.6 to 1.9 for autochthonous DOM (McKnight *et al*., 2001).

2.6. Data analyses

2.6.1. Parallel Factor Analysis (PARAFAC) modeling

EEMs were analyzed by applying PARAFAC, to identify the number, type and intensity of DOM fluorophores (Stedmon *et al*., 2003; Murphy *et al*., 2014). PARAFAC was performed including a total of 44 EEMs: 20 obtained from Lake Escondido samples and 24 from Lake Morenito. All the EEMs were corrected with the MATLAB toolbox drEEM (Murphy *et al*., 2013). The first approach involved visualization of each EEM and the removal of scatter peaks (i.e., Rayleigh and Raman), followed by an exploratory analysis using non-negative constraints to identify outliers. The number of components discriminated by PARAFAC was validated by split half analysis, applying random initialization (Murphy *et al*., 2013). Finally, excitation and emission loadings were used to localize the excitation and emission peaks of the components and their maximum intensity (F_{max}) (Murphy *et al*., 2013). The excitation and emission spectra for each component obtained through PARAFAC were queried against the fluorescence spectra of the open-access database OpenFluor (www.openfluor.org, Murphy *et al*., 2014), to determine coincidence with components reported in other studies. Components were assumed to be similar when a minimum similarity score of 0.95 was achieved.

2.6.2. Statistical analyses

The DOM parameters DOC, a_{440}, $SUVA_{254}$ and fluorescent components, as well as the Chl*a* concentration, conductivity and pH of lakes Morenito and Escondido were compared applying *t*-test or Mann-Whitney U tests.

One-way ANOVA was applied to study the effect of seasonality in both lakes, considering DOC concentrations and whole-lake DOC mass as well as CDOM and FDOM parameters. Post-hoc contrasts (Bonferroni) were performed to analyze the effect of seasonality within and between lakes. Linear regression analysis was applied to describe the relationship between a_{350}:DOC and $S_{275\text{-}295}$. Pearson correlation analyses were applied to study the relationship between HIX and BIX as well as between cumulative precipitation and CDOM and FDOM.

In order to analyze the effect of environmental factors on DOM features in lakes Morenito and Escondido, a redundancy analysis (RDA) was performed. The application of RDA was based on a previous detrended correspondence analysis (DCA), which indicated a linear distribution of the data set (ter Braak and Šmilauer, 1998). Two data matrices were considered in the RDA: one including DOM parameters (DOC, $S_{275\text{-}295}$, a_{350}:DOC, HIX, BIX and the fluorescent components C1, C2 and C3), and the other including environmental variables (cumulative precipitation, seasonal Q_{mv}, lake P:A, conductivity, Chl*a* concentration, fluence 150d , water temperature, and % Water). The analysis was performed using the CANOCO 4.5 software (ter Braak and Šmilauer, 1998), applying forward selection to evaluate the most influential environmental variables. The significance of the canonical axes was tested through Monte Carlo permutation tests (Leps and Šmilauer, 2003).

3. Results

3.1. Weather seasonality and inter-annual variations

During the three years studied, the precipitation regime, air temperature and solar radiation all showed the marked annual seasonality characteristic of the northern Patagonian region. Mean monthly cumulative precipitation varied between 1.8 and 400 mm, showing a clear pattern with alternating dry spring-summer periods (October to March) and wet fall-winter periods (April to September) (Figure 2A). As expected, dry periods were associated with higher temperature and PAR records and lower precipitation levels. In contrast, wet periods were characterized by low temperatures and PAR values and higher cumulative precipitation. These marked differences between dry and wet periods were reflected in the water level of both lakes (see below). Inter-annual fluctuations of the precipitation regime were also evident in the study period. Precipitation records indicated that the driest summer and the wettest winter occurred in 2015 (Figure 2A). The cumulative precipitation during winter was lowest in 2014, being ~30% lower than in 2013 and 2015. In 2015, summer precipitation was 45% and 24% lower than in 2013 and 2014, respectively.

The mean winter air temperature was 2.27 ± 2.61°C, with the lowest values between -6°C and -13°C. The mean air temperature in the summer was 9.62 ± 2.85°C, with the absolute maximum temperature peaking around 25°C to 32°C. The mean monthly PAR irradiance fluctuated around 0.19 ± 0.08 $\mu E\ cm^{-2}\ sec^{-1}$ in the winter and around 0.53 ± 0.12 $\mu E\ cm^{-2}\ sec^{-1}$ in the summer (Figure 2A). The cumulative precipitation 150 days before sampling ranged between 104 and 1297 mm (Figure 2B). The sampling periods in the lakes studied were representative of the end of the dry and wet seasons (see arrows in Figure 2B).

3.2. HGM and catchment features

The HGM parameters evaluated showed differences between the dry and wet seasons. Lake Morenito showed remarkable seasonal changes in its area, perimeter, volume, and depth, whereas Lake Escondido showed comparatively moderate seasonal fluctuations in HGM parameters (Table 1). During dry periods, both high evaporation and lower precipitation caused reduced water levels in both lakes; this phenomenon was also supported by a decrease in the water storage of the whole basin (Nahuel Huapi lacustrine system) (Figure 2B). In Lake Morenito, the water level changed up to 2 m between seasons, reflected in an increase in water volume (~52%), lake area (~ 24%) and perimeter (~25%) during the wet season (Table 1; Figure 1B,D). In contrast, in Lake Escondido, a smaller increase of ~ 0.5 m was observed in the water level, resulting in smaller seasonal changes in lake depth. The water volume of Lake Escondido during the wet season showed a moderate increase of ~13%, while the lake area and perimeter increased up to ~10.5% and ~19.5%, respectively (Table 1; Figure 1B,C). Regarding the P:A ratio, Lake Escondido showed overall higher values than Lake Morenito, implying a comparatively greater contact between the lake and the terrestrial environment. Nevertheless, the P:A ratio was higher during the wet season in both lakes. The drainage area of Lake Morenito was 3.5 times greater than that of Lake Escondido, while the drainage ratio was similar in both lakes during the wet season, when rainwater drains from the catchment (Table 1). The subcatchments of both lakes have dense forest cover, and a small residential area in the case of Lake Morenito (Table 1). The % Water fluctuated between 3.57 and 7.63 % in Lake Morenito, and was null in Lake Escondido due to the absence of other water bodies in the catchment.

The comparison of hypsographic curves between lakes and seasons revealed clear seasonal differences in several HGM features. Lake Morenito presents higher lake area, depth and volume than Lake Escondido, as well as higher seasonal variation in these parameters (Table 1; Supporting Figure S1). Despite these differences, both lakes showed similar mean annual WRT, although the mean annual water discharge (Q_{mv}) was 2.7 fold higher in Lake Morenito than in Lake Escondido (Table 1). The analysis of seasonal Q_{mv} showed an increase in water discharge towards the wet season and stagnation during the dry season in both lakes (Table 1).

3.3. Limnological parameters, DOC and CDOM characterization and seasonality

A comparative analysis between the lakes studied showed that mean conductivity was significantly higher in Lake Morenito (72.1 ± 4.2 µS cm^{-1}) than in Lake Escondido (62.8 ± 2.1 µS cm^{-1}; t=2.78, p=0.009), whereas the pH was similar in both lakes (*t*- test, p>0.05), ranging between 6.3 and 8.0. The water temperature was significantly lower in Lake Morenito (12.3 ± 3.1 °C) than in Lake Escondido (14.5 ± 1.8 °C; t=709.0; p=0.004). The water column was thermally homogenous in both lakes on all sampling dates (p> 0.05). The mean Chl*a* concentration was similar in both lakes (1.51 ± 1.22 µg L^{-1} in Lake Morenito and 1.22 ± 0.33 µg L^{-1} in Lake Escondido; *t*- test, p>0.05). The mean DOC concentration was significantly higher in Lake Escondido (3.82 ± 0.28 mg L^{-1}) than in Lake Morenito (2.97 ± 0.20 mg L^{-1}) (t=-12.58, p<0.001). The mean CDOM absorption coefficients (i.e., a_{350} and a_{440}) were also significantly higher in Lake Escondido than in Lake Morenito. For instance, water color (a_{440}) was 1.8 fold higher in Lake Escondido (0.95 ± 0.4 m^{-1}) than in Lake Morenito (0.52 ± 0.16 m^{-1}; t=-5.17, p<0.001). $SUVA_{254}$ indicated a higher DOM aromaticity in Lake Escondido (5.79 ± 1.06 L mg^{-1} m^{-1}) than in Lake Morenito (4.52 ± 0.74 L mg^{-1} m^{-1}) (t=-4.98, p<0.001). The relationship between DOC concentration and conductivity was fitted to a linear model, resulting in a significant positive trend in the case of Lake Morenito (R^2 =0.56; p <0.001, n= 24) and in a non-significant relationship in Lake Escondido (p >0.05).

Regarding the analysis of within-lake and between-lake DOM variability consistent differences in concentration and quality parameters were observed during the three years studied. Both lakes showed significant differences in mean DOC concentrations between seasons. In Lake Escondido, DOC concentration decreased towards the dry season (Table 2), whereas Lake Morenito showed the opposite pattern, with significantly higher mean DOC values during the dry season (one-way ANOVA, $p<0.001$; Table 2; Figure 3A). Conversely, when whole-lake DOC masses were incorporated into the seasonal analysis, a significant decrease towards the dry season was found in both lakes, indicating a lower bulk of DOM for this season (Table 2; Figure 3B). In this scenario, DOC mass showed a synchronous pattern between lakes ($r= 0.85$; $p< 0.001$), whereas the variation in DOC concentration showed an asynchronous pattern between lakes ($p> 0.05$). This suggests that DOC analysis based solely on DOC concentration could hinder the behavior of the whole-lake DOC mass pattern (Figure 3A,B). The importance of the marked seasonal changes in lake volume and the interaction of concentration/dilution processes behind the observed pattern of DOC concentration in Lake Morenito are discussed in Section 4.2.

CDOM also presented clear seasonality, with significantly higher mean a_{350} values during the wet season in both lakes (one-way ANOVA, $p< 0.001$, Table 2, Figure 4). Lake Escondido always presented higher a_{350} mean values than Lake Morenito, although no significant differences were found between the dry season of the former and the wet season of the latter. Analysis of the relationship between DOC concentration and CDOM showed contrasting patterns between lakes. Lake Morenito showed a decrease in a_{350} with high values of DOC concentration, whereas Lake Escondido showed an increase in a_{350} with high DOC concentration (Figures 3A and 4).

Seasonality was also recorded in other optical metrics such as water color (a_{440}) aromaticity ($SUVA_{254}$), lignin content (a_{350}:DOC) and spectral slope ($S_{275-295}$), both within and between lakes (one-way ANOVA, $p<0.001$; Table 2). The lakes showed lower values of a_{440}, $SUVA_{254}$, lignin content and molecular weight (higher mean values of $S_{275-295}$) during the dry season (Table 2). In general, optical parameters as a_{440}, $SUVA_{254}$ and a_{350}:DOC were significantly higher in Lake Escondido than in Lake Morenito during the wet season. However, the differences in a_{440} and $SUVA_{254}$ observed between the dry season of Lake Escondido and the wet season of Lake Morenito were not significant (Table 2).

Overall, the temporal variation of several DOM spectrophotometric parameters fluctuated synchronously between lakes throughout the study period. Considering the entire data set, significant correlations were observed between lakes for: a_{440} ($r = 0.91$, $p< 0.0001$), $SUVA_{254}$ ($r = 0.89$, $p< 0.0001$), a_{350}:DOC ($r = 0.95$, $p< 0.0001$) and $S_{275-295}$ ($r = 0.98$, $p< 0.0001$). These relationships revealed similar seasonal trends between lakes, indicating the existence of external drivers controlling DOM properties.

The relationship between a_{350}:DOC and $S_{275–295}$ showed a strong negative pattern ($R^2 = 0.88$; $p< 0.001$; $n= 44$) along a decreasing precipitation gradient (Figure 5A, see color scale for precipitation values). In fact, this relationship was coupled with cumulative precipitation before sampling, showing that seasonal and inter-annual rainfall variation affects CDOM optical parameters and is reflected in DOM quality changes (Figure 5A). Indeed, several CDOM properties strongly correlated with cumulative precipitation, either positively (a_{350}:DOC and a_{440}) or negatively ($S_{275-295}$) (Supp. Table 1). Across the seasonal precipitation gradient, higher values of a_{350}:DOC and lower values of $S_{275–295}$ were observed during the wet season in both lakes, probably indicative of fresher terrestrial DOM inputs. Inter-annual variation between wet seasons was observed in both lakes, with greater signs of terrestrial DOM (low $S_{275-295}$ and high a_{350}:DOC values) in rainy years (i.e., 2015 and 2013 > than 2014) (Figure 5A). During the dry season, both lakes showed highest values of $S_{275–295}$ and lowest lignin content (Figure 5A), revealing the impact of DOM transformation processes during this period (probably due to interaction between higher photochemical processing and lower water discharge, see Discussion section 4.3). In addition, low inter-annual variation of DOM properties was observed during the dry period in both lakes.

3.4. FDOM characterization

HIX values exhibited significant seasonal variations in both lakes, with higher predominance of humic compounds in the wet season (one-way ANOVA, $p< 0.001$; Table 2). The mean HIX values for the wet season were always significantly higher in Lake Escondido than in Lake Morenito, regardless of the season (Table 2). FI values were similar in both lakes (1.51 ± 0.11 and 1.49 ± 0.09 in Lake Morenito and Lake Escondido, respectively; t- test, $p>0.05$) irrespective of the season.

BIX values also showed seasonal differences in both lakes (one-way ANOVA, $p<0.001$; Table 2), with higher values during the dry season than during the wet season (Figure 5B). However, BIX values were always <0.75, indicating low autochthonous production of DOM. Comparing lakes on a seasonal basis, Lake Escondido always presented less autochthonous and more humified DOM than Lake Morenito (Table 2; Figure 5B). BIX and HIX were negatively correlated ($r=-0.86$, $p<0.001$, $n=44$) and, as previously found for CDOM parameters, BIX and HIX were significantly and positively correlated with cumulative precipitation ($r=-0.67$, $p<0.001$; $r=0.49$, $p<0.001$, BIX and HIX respectively; Supp. Table S1).

The PARAFAC analysis of the EEM spectra identified three fluorescent components (C1, C2 and C3) that contributed to the total FDOM in the two lakes studied (Table 3). C1 has a primary excitation (Ex) peak at 240 nm and a secondary peak at 305 nm, with a maximum emission (Em) peak at 396 nm, and is often referred to as a combined component constituted by the A + M peaks (Yamashita *et al*., 2010; Cawley *et al*., 2012). C2 has a primary Ex maximum at 240 nm and a secondary Ex peak at 345 nm, showing an Em peak at 460 nm, referred to as the A + C peaks (Yamashita *et al*., 2010; Shutova *et al*., 2014). C3 has a primary Ex maximum at 240 nm and a secondary Ex at 280 nm, with an Em at 361.5 nm, and has been associated with Tryptophan-like fluorophore (T-peak) (Garcia *et al*., 2015b; Table 3).

The intensity of fluorescent components showed a regular pattern in both lakes during the three years studied. The humic component C1, followed by component C2, was predominant, whereas the non-humic component C3 identified in both lakes had a relatively lower proportion (Table 2). C1 and C2 presented higher values in Lake Escondido (Mann–Whitney U-test; $p<0.001$), whereas C3 was similar in both lakes (Mann–Whitney U-test; $p=0.82$) (Figure 6A,B,C).

The seasonal analysis of component intensities exhibited significant within-lake and between-lakes variation for C1 and C2 (one-way ANOVA, $p<0.001$; Table 2). However, C3 only showed significant differences within each lake (Table 2). A substantial decrease in C2 during the dry season (39 and 42%) and a less pronounced decrease in C1 (13 and 18%) were observed in lakes Morenito and Escondido, respectively. Concomitantly, mean values of C3 increased around 14 and 27% towards the dry season in lakes Morenito and Escondido, respectively.

Overall, C2 showed strong synchronous variation throughout the study period in both lakes, as indicated by their strong correlation ($r=0.93$; $p<0.0001$). C1 and C3 also displayed similar trends between lakes, but the correlations were comparatively lower ($r=0.56$; $p=0.01$, and $r=0.55$; $p=0.02$, for C1 and C3, respectively).

Regarding the relative contribution of fluorescent components (as a percentage $\%C_i$), C1 showed the lowest variation between seasons in both lakes, with a slight increase (6%) towards the dry season (Table 2, Figure 6D). In contrast, C2 exhibited a significant decrease (25%) during the dry season in both lakes (one-way ANOVA, $p<0.001$) (Table 2; Figure 6E). C3 showed the highest proportional variation, with a significant increase of 27 and 40% towards the dry season in Lake Morenito and Lake Escondido, respectively (one-way ANOVA, $p<0.001$) (Table 2, Figure 6F).

The spectral slope ($S_{275\text{-}295}$) was strongly negatively correlated with %C2 ($r= -0.82$; $p<0.0001$; $n=44$; Figure 6E), and a positively related to %C3 ($r= 0.84$; $p<0.0001$; $n=44$, Figure 6F). The pattern observed during the dry season can be summarized as a decrease in humic C2 and a concomitant increase in C3, reflecting a transition from high to low molecular weight DOM. These results indicate the transformation of DOM and the occurrence of by-products of this process during the dry season. The opposite pattern observed in the wet season probably indicates the influence of terrestrial DOM inputs due to increased runoff.

The component C2 was positively linked with cumulative precipitation (r=0.49; p<0.001), whereas C3 presented the opposite pattern (r= -0.52, p<0.001) (Supp. Table S1). In contrast, in the case of C1, the relationship was not significant (p> 0.05). The relative contribution of the fluorescent components and precipitation showed a negative relationship in the cases of C1 and C3 (r= -0.38; p= 0.02; r= -0.50; p<0.001, respectively), and a positive trend with C2 (r= 0.61; p<0.001).

3.5. Multivariate redundancy analysis (RDA)

RDA was conducted with DOC concentration and DOM properties as response variables and environmental variables as explanatory ones. Six out of the eight environmental variables considered were included in the model by forward selection (cumulative precipitation, P:A, fluence 150d, % Water, Chl*a* and water temperature). The first and second canonical axes explained 97.9% of the total observed variation (axis 1= 95.6%; axis 2= 2.3%). The Monte Carlo unrestricted permutation test on the first eigenvalue indicated that the environmental variables were significantly correlated with the first axis (p =0.002) as well as with all the canonical axes (p =0.002). Precipitation and fluence 150d separated the wet and the dry seasons, whereas P:A separated Lake Morenito from Lake Escondido. Samples from the wet season showed high values of DOC, a_{350}:DOC, HIX, C1 and C2, while those of the dry season displayed higher values of $S_{275\text{-}295}$, C3 and BIX (Figure 7).

4. Discussion

4.1. Precipitation conditions and HGM features

Cumulative precipitation showed strong seasonality during the three years studied despite the inter-annual variability detected in precipitation volume. Such a strong seasonal pattern, with precipitation concentrated in the fall-winter period, coincides with the general precipitation regime described for North Patagonia, reflecting the effect of the South Pacific anticyclone oscillation southwards in summer and northwards in winter (Paruelo *et al*., 1998; Barros *et al*., 2015).

Regarding the analysis of the HGM features, the higher P:A ratio of Lake Escondido compared to Lake Morenito is associated with its smaller surface area, which implies greater interaction with the terrestrial environment (Figure 7) (Wetzel, 2001; Webster *et al*., 2008; Gerea *et al*., 2016). Lakes with high P:A receive relatively high inputs of terrestrial matter compared to lakes with lower P:A ratios (Wetzel, 2001; Webster *et al*., 2008). The high P:A ratio for smaller lakes results in high contact surface with the surrounding landscape (Hanson *et* *al*., 2007). A more detailed analysis of HGM features showed clear differences between lakes in their catchment size, Q_{mv} values and water level fluctuations. However, the greater volume of Lake Morenito counteracted its higher Q_{mv}, which explains their similar annual WRT. In addition, the landscape position of the lakes results in a differential degree of connectivity with other water bodies, as Lake Morenito belongs to a chained lacustrine system while Lake Escondido is unique in its basin. In this context, the increase in water level during the wet season (up to 2 m) enhances the connectivity of Lake Morenito with adjacent lakes (Figure 1), up to the point of experiencing possible refluxes from the deep Lake Moreno West, as previously described for this chained system (Rapacioli, 2011). In contrast, the dry period promotes stagnant conditions in both lakes (low Q_{mv}), due to lower precipitation and enhanced evaporation (Figure 7). These particular patterns led us to assume seasonal differences in WRT in these lakes, being shorter during the wet period and longer during the dry period (see Kellerman *et al*., 2015). In the future, these differential hydrological scenarios would be further considered to determine the variability of DOM quantity and quality in the lakes studied (Figure 7).

4.2. Influence of hydrological conditions on the seasonal variation of DOC concentration

It is generally well accepted that precipitation events promote greater connectivity and runoff, and consequently, mobilization of terrestrial DOM from the topsoil to adjacent aquatic systems, which increases their DOC concentrations (Van Gaelen *et al*., 2014). However, the lakes studied showed contrasting patterns of DOC concentration. In Lake Escondido, DOC concentrations were higher in the wet season than in the dry season, whereas in Lake Morenito, DOC was significantly higher during the dry season. However, when the variability of the whole-lake DOC mass was analyzed, a significant increase towards the wet season was observed in both lakes, indicating a greater DOM pool during this period. We hypothesize that the unexpected pattern of DOC concentration in Lake Morenito may be related to its greater fluctuation in water level between seasons, which implied the loss of ca. 50% lake volume towards the dry season. This important water loss goes together with the loss of connectivity of Lake Morenito with adjacent water bodies. During the wet season, the high water level promotes greater connectivity, with a potential for reflux of very low DOC water (ca. 0.6 mg L^{-1}) from the deep ultraoligotrophic Lake Moreno West into Lake Morenito, which may cause a dilution effect (Morris *et al*., 1995; Rapacioli, 2011). During the dry season, the absence of water inputs and the incidence of strong evaporation may explain the drastic decrease in water level, also reflected in higher DOC concentrations. This assumption was supported by the positive correlation found between DOC concentration and conductivity in Lake Morenito, as has also been observed by Anderson and Stedmon (2007) in shallow lakes of Greenland. Thus, the DOC analysis based exclusively on DOC concentration may not reflect the actual behavior of whole-lake DOC mass (Figure 3A,B). These results highlight the importance of integrating the influence of climate, the catchment, and the hydrological network with in-lake processes to account for the spatial and temporal variability of DOM, as suggested by Kothawala *et al*. (2014).

4.3. CDOM and FDOM optical properties: Interactive effects of weather and hydrogeomorphic features

In general, DOM quality parameters showed clear seasonal differences associated with contrasting DOM drivers (allochthonous inputs vs. in-lake degradation processes). The differences in DOM properties observed between lakes were found to be related to the particular HGM features of each lake.

In the wet season, the DOM pool was characterized by high values of CDOM (a_{350}, a_{440}), high aromaticity ($SUVA_{254}$), lignin content (a_{350}:DOC) and molecular weight ($S_{275\text{-}295}$), relating significantly to precipitation (Supp. Table 1). In accordance with this, these properties were associated with higher inputs of fresh terrestrial DOM during the wet season and displayed a lower degree of internal processing. In fact, this period was characterized by fast flow paths (higher Q_{mv}) leading to a shorter WRT, a condition known to dampen microbial processing (Köhler *et al*., 2013). The strong terrigenous signatures recorded during the wet season were also shown by the significant inverse relationships between a_{350}:DOC and $S_{275\text{-}295}$ along a decreasing precipitation gradient (Figure 5A, upper left corner; Figure 7). Indeed, in both lakes, during the rainy years 2013 and 2015, the CDOM properties indicated DOM of higher molecular weight and lignin content in comparison with the drier 2014, clearly reflecting inter-annual differences in cumulative precipitation.

A loss of DOM was observed in the dry period, associated with changes in CDOM quantity and properties. In both lakes, less absorptive DOM and a progressive decrease in molecular weight was observed towards the dry period (Figure 5A, lower right corner). We hypothesized that photodegradation is the main driver of DOM transformation during the dry period, through the combined effect of high irradiance and water shortage, leading to very low Q_{mv} and long WRT (Figure 7). This assumption is supported by previous empirical evidence of the photobleaching effect both in the lakes studied (Diéguez *et al*., 2013) and in other aquatic systems (Anderson and Stedmon, 2007; Helms *et al*., 2008; Fichot and Benner, 2012).

Regarding inter-annual variation, CDOM parameters showed higher similarity among dry periods than among wet periods. Apparently, the longer WRT and the high exposure to photobleaching led to homogenization of the CDOM properties, independently of the DOM inputs received during the previous wet season. In fact, in Andean Patagonia, the high influence of solar radiation during spring-summer has long been acknowledged as a major factor influencing CDOM properties, due to the combination of temperate latitude, altitude and a dry limpid atmosphere (Zagarese *et al*., 1998).

Consistent results were obtained from the FDOM characterization, with higher intensity values of the humic fluorescent components C1 and C2 in the wet period (Table 2; Figure 6A,B; Figure 7). These humic components have been related to terrestrial sources and their dynamics are influenced by hydrological conditions, especially runoff inflows (Stedmon and Markager, 2005; Zhou *et al*., 2015). In addition, the highest HIX values were found during the wet period (Table 2; Figure 5). In particular, C2 and HIX were significantly and positively related to precipitation, while C1 showed a positive trend, though not significant (Supp. Table 1; Figure 7). In general, terrestrial DOM inputs associated with precipitation have a high content of stable aromatic structures, containing lignin compounds which are biopolymers found exclusively within terrestrial vascular plants, and are related to humic C2 (Kalbitz *et al*., 2003; Hernes *et al*., 2009; Stubbins *et al*., 2010). Furthermore, the humic component C1 has been associated with microbially transformed products derived from terrestrial organic substances (Stedmon and Markager, 2005; Zhang *et al*., 2010; Zhou *et al*., 2015). Such products may also be produced in soils; in particular, C1 has been described as a microbially degraded humic-like component associated with water-extractable soil organic matter (Wei *et al*., 2015). This evidence explains the terrestrial signature of C1 observed in the two shallow lakes studied. In addition, the non-humic C3 has been associated with the photochemical and/or biological processing of DOM (Maie *et al*., 2007; Fellman *et al*., 2010; Lapierre *et al*., 2013). The low contribution of this component during the wet season could be attributable to the high Q_{mv} recorded in both lakes, which could decrease in-lake DOM production and/or processing.

The effects of photobleaching were also detectable through the loss of FDOM and the transformation of fluorophores, as noted in several studies (Reche *et al*., 1999; Moran *et al*., 2000; Twardowsky and Donaghay, 2001). During the present short-term study, the intensity and percentage of C2 decreased significantly, and in a greater proportion than C1 during the dry season, with a concomitant increase in C3 (Figure 7). The higher intensity and percent contribution of C3 and the longer WRT exhibited during the dry season suggest that C3 may be a persistent component, being renewed constantly at the expense of other components. Indeed, C3 is, at least partially, a subproduct of photodegradation of the humic C2, as has been shown in photobleaching experiments performed in the same lakes (Diéguez *et al*., 2013) and also observed in other studies (Maie *et al*., 2007; Hernes et al 2009). Autochthonous microbial and/or algal production has been also considered to explain C3 occurrence (e.g., Coble, 2007; Kothawala *et al*., 2014). However, we disregarded the dominance of the autochthonous origin of DOM in the lakes studied because bacterial and primary production was low, in agreement with their oligotrophic condition (Bastidas Navarro *et al*., 2009). Furthermore, this assumption is supported by the low BIX values (< 0.75), indicative of a low DOM autochthonous production (Huguet *et al*., 2009), even in the dry period (Figure 5B). Concerning C1 (as %), lower differences between seasons, with a small increase during the dry period, were observed. So, C1 appears to be more photo-resistant than C2 (Figure 6D,E). Other studies have shown that peak C (analogous to our C2) may shift to peak M (analogous to our C1; see Table 3), suggesting that C1 could be a mixture of intermediate compounds less susceptible to photodegradation (Chari *et al*., 2012; Ishii and Boyer, 2012; Helms *et al*., 2013). However, all these processes take place simultaneously, making it difficult to assign a directional change in the case of C1.

In relation to the FI values, the differences observed between seasons and lakes were not significant. Thus, this index cannot be considered a sensitive proxy to track differences like HIX and BIX, as reported previously for oligotrophic mountain lakes and streams of the region (Garcia *et al*., 2015a, b).

The marked synchronicity observed in several CDOM and FDOM properties and whole-lake DOC masses indicates a similar response to the climate forcing operating at this latitude and provides a framework to understand the functioning of shallow Andean lakes in a landscape. Nevertheless, the intensity of the response was different between lakes as a function of their differences in HGM features. Within-lake differences were the result of contrasting seasonal patterns in precipitation and fluence 150d, which influenced in-lake processes (e.g., DOM degradation), whereas the differences between lakes were due to their differential HGM features (e.g., P:A) and hydrological connectivity. These results were integrated and summarized by the RDA (Figure 7).

Remarkably, DOC concentration appeared as an unresponsive variable to climate-driven forces in Lake Morenito, due to its particular hydrological condition, seasonal differential connectivity and strong evapoconcentration processes.

4.4. Ecological implications of DOM variability and potential impacts of predicted climate scenarios

The DOM pool affects many ecological processes in aquatic systems (Wetzel, 2001), and its influence on nutrient availability is central. In particular, DOM is strongly associated with the nitrogen (N) cycle through the dissolved organic N (DON) fraction (Bronk *et al*., 2007), since both humic and non-humic organic substances may contain different numbers of N atoms in their structure (Stubbins *et al*., 2014). In temperate forests of South America, the loss of N occurs through the export of DON concomitantly with precipitation (Perakis and Hedin, 2002). Therefore, in North Patagonia, the strong seasonality and the inter-annual variability in precipitation could differentially affect N availability in aquatic systems. DON compounds are assimilated by bacteria and/or phytoplanktonic organisms (Bronk *et al*., 2007), and thus, are likely to induce cascading effects in aquatic food webs. On the other hand, CDOM plays a central ecological role in regulating the underwater light climate of lakes (Wetzel, 2001), especially in oligotrophic systems (Bukaveckas and Robbins-Forbes, 2000). In fact, in lakes Morenito and Escondido, CDOM determines the differential spectral composition of underwater irradiance, which in turn influences the structure of their phytoplankton communities (Gerea *et al*., 2016). CDOM comprises major optically active substances that absorb UV radiation, modulating the effects of UV on planktonic organisms (Sommaruga and Augustin, 2006). Patagonian lakes are naturally exposed to high UV radiation levels due to their latitude, altitude and pristine atmospheric conditions. These, along with the extreme transparency of the water, create harsh radiation conditions in the upper layers of deep lakes and even in the whole water column in shallow lakes (Zagarese *et al*., 2001). In relation to the UV impact on DOM quality, our results showed the photochemical transformation of CDOM and FDOM during the dry season, for example decreasing DOM molecular weight and influencing the relative contribution of the fluorescent components C2 and C3 (Figure 6E,F). In addition, the transformation of C2 to C3 and the higher biodegradability of C3 may enhance the availability of C for the microbial food web during the dry season (Guillemette and del Giorgio, 2011; Lapierre *et al*., 2013). Indeed, the phototransformation of DOM results in a more labile pool for heterotrophic uptake (Hiriart-Baer *et al.*, 2008). Thus, photochemical degradation processes like those detected during the dry season may have a strong impact on the trophic dynamics of Andean Patagonian oligotrophic lakes, in which microbial food webs and primary production are dominated by mixotrophic organisms (Bastidas Navarro *et al*., 2009; Gerea *et al*., 2016).

The quality and concentration of DOM in freshwater systems also control metal-ligand interactions (Aiken, 2014), determining the toxicity and availability of mercury (Hg) for bioaccumulation and bioconcentration in aquatic food webs (Ravichandran, 2004; Luengen *et al*., 2012). In Andean Patagonian lakes, low DOC and high total Hg (THg) concentration determine high THg:DOC ratios, promoting extremely high availability of Hg to bind biotic and abiotic particles (Ribeiro Guevara *et al.*, 2008; Soto Cárdenas *et al*., 2014; Soto Cárdenas *et al.*, *in prep.*), which are transferred to higher trophic levels or different trophic compartments (Arribére et al., 2010; Rizzo et al., 2011; 2014). Moreover, in these lakes, DOM quality has been shown to affect the Hg adsorption to planktonic organisms (Soto Cárdenas, 2015). Higher concentrations of CDOM and humic DOM in natural water of different lakes, including Lakes Morenito and Escondido, have been found to slow down the adsorption of Hg in planktonic algae and herbivorous zooplankton. Whereas lower CDOM levels and photodegraded DOM have been found to enhance the bioavailability of Hg (Diéguez *et al*., 2013). In Andean lakes of Patagonia, DOM-Hg interactions via complexation and/or photochemical reactions determine the speciation and mobility of Hg among different ecosystem compartments and within the catchment (Soto Cárdenas *et al.*, *in prep.*). Considering the results of the present study, the seasonal differences in DOM concentration and quality in lakes Morenito and Escondido would likely reflect in seasonal changes in Hg bioavailability within and between lakes. Hence, understanding the factors driving the DOM pool on temporal and spatial scales allows predicting pathways of Hg mobility and bioavailability in Andean Patagonian lakes.

Predictions of climate change for the Andean North Patagonian region anticipate a sustained decrease in winter precipitation (Garreaud *et al.*, 2013; Barros *et al.*, 2015), which would diminish hydrological connectivity among lakes and between the lakes and their surroundings, with a consequent reduction in terrestrial inputs into aquatic systems. In the forecasted regional climate scenario, a decrease in the allochthonous subsidies of organic C and N could lead to higher water transparency and UV exposure, structural and functional changes in aquatic communities, and higher Hg bioavailability, as well as other unforeseen environmental changes. The predicted DOM pattern contrasts with the trend observed in the Northern Hemisphere, where the strong transference of C from catchments is causing the browning of inland water bodies (e.g., Monteith *et al.*, 2007; Larsen *et al.*, 2011; Thrane *et al.*, 2014).

Overall, our results provide evidence of the complex interplay between climate, landscape, and hydrogeomorphic variables in temperate shallow lakes of the Southern Hemisphere.

5. Conclusions

- The variation in whole-lake DOC mass and CDOM and FDOM properties showed marked synchronicity in the two lakes studied, indicating a similar response to the climate-driven forces operating at this latitude. In contrast, the intensity of the response in terms of DOC concentration was different between lakes, according to their particular HGM features and hydrological connectivity.
- The lower DOC concentration found during the wet period (fall-winter) compared to the dry period (spring-summer) can be attributed to an intense dilution/evapoconcentration process in Lake Morenito.
- Precipitation and runoff increased Q_{mv}, water level and terrestrial inputs of highly aromatic, humic and high molecular size DOM during the wet season in both lakes.
- Photodegradation was the main driver of DOM transformation towards the dry season, due to the combined effect of high irradiance and longer WRT, resulting in less absorptive DOM and a progressive decrease in molecular weight.
- During wet periods, inter-annual variation in CDOM and FDOM parameters showed clear differences associated with differential cumulative precipitation. In contrast, during dry periods, DOM properties were homogeneous as a result of stagnant conditions.

Our results revealed that DOM quality parameters, together with whole-lake DOC mass, are sensitive to climate forcing, allowing an accurate assessment of C dynamics in these shallow temperate lakes. The HGM features of the lakes modulated the intensity of the response, and therefore must be taken into account for an appropriate assessment of DOM variability. Changes in DOM quality may have profound implications for biogeochemical processes, but may not always be reflected in DOC concentration. Understanding the forces driving seasonal and inter-annual dynamics of DOM and their effect on C cycling is necessary to infer potential pathway changes in temperate lakes of Patagonia, due to the climate scenario anticipated for this century.

Acknowledgements

We are grateful to the San Carlos de Bariloche Town Council for granting permission to sample lakes within its jurisdiction, and to the two anonymous reviewers whose comments helped us to improve this manuscript. We especially thank Dr. Horacio Zagarese for his valuable comments on an early version of the manuscript. Victoria González Eusevi and Audrey Shaw are especially acknowledged for the revision of the English language. This investigation was funded by Agencia Nacional de Promoción Científica y Técnica (PICT 2012-1200; PICT 2013-1384; PICT 2015-3496) and by Universidad Nacional del Comahue (UNC 04/B194). Carolina Soto Cárdenas and Marina Gerea were supported by CONICET fellowships. Patricia E. Garcia, Gonzalo L. Pérez, María C. Diéguez, Mariana Reissig and Claudia Queimaliños are CONICET researchers (Argentina).

References

Adrian R, O'Reilly CM, Zagarese H, Baines SB, Hessen DO, Keller W, Livingstone DM, Sommaruga R, Straile D, Van Donk E, Weyhenmeyer GA, Winder M. 2009. Lakes as sentinels of climate change. *Limnology and Oceanography* **54**: 2283–2297.

AIC. 2015. Informes Hidrometeorológicos 2012–2015. Río Negro, Argentina: Autoridad Interjurisdiccional de Cuencas.

Aiken GR. 2014. Fluorescence and Dissolved Organic Matter: A Chemist's Perspective. In *Aquatic Organic Matter Fluorescence*, Coble P, Lead J, Baker A, Reynolds DM, Spencer RGM (eds). Cambridge University Press: New York; 35-74.

Anderson NJ, Stedmon CA. 2007. The effect of evapoconcentration on dissolved organic carbon concentration and quality in lakes of SW Greenland. *Freshwater Biology* **52**: 280-289.

Arribére M, Diéguez MC, Ribeiro Guevara S, Queimaliños CP, Fajon V, Reissig M, Horvat M. 2010. Mercury in an ultraoligotrophic North Patagonian Andean lake (Argentina): concentration patterns in different components of the water column. *Journal of Environmental Sciences* 22: 1171–1178.

Barros VR, Boninsegna JA, Camilloni IA, Chidiak M, Magrín GO, Rusticucci M. 2015. Climate change in Argentina: trends, projections, impacts and adaptation. *WIREs Climate Change* **6**: 151-169.

Bastidas Navarro M, Balseiro E, Modenutti BE. 2009. Effect of UVR on lake water and macrophyte leachates in shallow Andean-Patagonian lakes: bacterial response to changes in optical features. *Photochemistry and Photobiology* **85:** 332–340.

Bertilsson S, Tranvik LJ. 2000. Photochemical transformation of dissolved organic matter in lakes. *Limnology and Oceanography* **4**: 458–463.

Bianchi E, Villalba R, Viale M, Couvreux F, Marticorena R. 2016. New precipitation and temperature grids for Northern Patagonia: Advances in relation to Global Climate grids. *Journal of Meteorological Research* **30**: 38-52.

Bronk DA, See JH, Bradley P, Killberg L. 2007. DON as a source of bioavailable nitrogen for phytoplankton. *Biogeosciences* **4**: 283-296.

Bukaveckas PA, Robbins-Forbes M. 2000. Role of dissolved organic carbon in the attenuation of photosynthetically active and ultraviolet radiation in Adirondack lakes. *Freshwater Biology* **43**: 339-354.

Cawley KM, Ding Y, Fourqurean J, Jaffé R. 2012. Characterising the sources and fate of dissolved organic matter in Shark Bay, Australia: a preliminary study using optical properties and stable carbon isotopes. *Marine and Freshwater Research* **63**: 1098-1107.

Chari NVHK, Sarma NS, Pandi SR, Murthy KN. 2012. Seasonal and spatial constraints of fluorophores in the midwestern Bay of Bengal by PARAFAC analysis of excitation emission matrix spectra. *Estuarine, Coastal and Shelf Science* **100**: 162-171.

Coble PG. 2007. Marine optical biogeochemistry: the chemistry of ocean color. *Chemical Reviews* **107**: 402-418.

Del Vecchio R, Blough NV. 2004. On the Origin of the Optical Properties of Humic Substances. *Environmental Sciences and Technology* **38**: 3885-3891.

Díaz SB, Booth CR, Smolskaia I. 1994. Effects of ozone depletion on irradiances and biological doses over Ushuaia. Archiv für Hydrobiologie–Beiheft Ergebnisse der Limnologie 43: 115–122.

Diéguez MC, Queimaliños CP, Ribeiro Guevara S, Marvin-DiPasquale M, Soto Cárdenas C, Arribére MA. 2013. Influence of dissolved organic matter character on mercury incorporation by planktonic organisms: An experimental study using oligotrophic water from Patagonian lakes. *Journal of Environmental Sciences* **25:** 1980-1991.

Downing JA, Prairie YT, Cole JJ, Duarte CM, Tranvik LJ, Striegl RG, McDowell WH, Kortelainen P, Caraco NF, Melack JM. 2006. The global abundance and size distribution of lakes, ponds, and impoundments. *Limnology and Oceanography* **51**: 2388-2397.

Erlandsson M, Buffam I, Folster J, Laudon H, Temnerud J, Weyhenmeyer GA, Bishop K. 2008. Thirty-five years of synchrony in the organic matter concentrations of Swedish rivers explained by variation in flow and sulphate. *Global Change Biology* **14:** 1191-1198.

Evans CD, Chapman PJ, Clark JM, Monteith DT, Cresser MS. 2006. Alternative explanations for rising dissolved organic carbon export from organic soils. *Global Change Biology* **12**: 2044-2053.

Fellman JB, Hood E, Spencer RGM. 2010. Fluorescence spectroscopy opens new windows into dissolved organic matter dynamics in freshwater ecosystems: A review. *Limnology and Oceanography* **55(6)**: 2452-2462.

Fichot CG, Benner R. 2012. The spectral slope coefficient of chromophoric dissolved organic matter ($S_{275–295}$) as a tracer of terrigenous dissolved organic carbon in river-influenced ocean margins. *Limnology and Oceanography* **57:** 1453-1466.

García PE, Diéguez MC, Queimaliños CP. 2015a. Landscape integration of North Patagonian mountain lakes: a first approach using the characterization of dissolved organic matter. *Lakes and Reservoirs: Research and Management* **20**: 19-32.

Garcia RD, Reissig M, Queimaliños CP, Garcia PE, Diéguez MC. 2015b. Climate-driven terrestrial inputs in ultraoligotrophic mountain streams of Andean Patagonia revealed through chromophoric and fluorescent dissolved organic matter. *Science of the Total Environment* **521**: 280-292.

Garreaud R, López P, Minvielle M, Rojas M. 2013. Large-scale control on the Patagonian climate. *Journal of Climate* **26**: 215-230.

Gerea M, Pérez G, Unrein F, Soto Cárdenas C, Morris D, Queimaliños C. 2016. CDOM and the underwater light climate in two shallow North Patagonian lakes: evaluating the effects on nano and microphytoplankton community structure. *Aquatic Sciences.* DOI: 10.1007/s00027-016-0493-0.

Guillemette F, del Giorgio PA. 2011. Reconstructing the various facets of dissolved organic carbon bioavailability in freshwater ecosystems. *Limnology and Oceanography* **56**: 734–48.

Häder DP, Kumar HD, Smith RC, Worrest RC. 2007. Effects of solar UV radiation on aquatic ecosystems and interactions with climate change. *Photochemical and Photobiological Sciences* **6**: 267-285.

Häder DP, Williamson CE, Wängberg S-Å, Rautio M, Rose KC, Gao K, Helbling EW, Sinha RP, Worrest R. 2015. Effects of UV radiation on aquatic ecosystems and interactions with other environmental factors. *Photochemical and Photobiological Sciences* **14**: 108-126.

Håkanson L. 2005. The importance of lake morphometry and catchment characteristics in limnology – ranking based on statistical analyses. *Hydrobiologia* **541**: 117-37.

Hanson PC, Carpenter SR, Cardille JA, Coe MT, Winslow LA. 2007. Small lakes dominate a random sample of regional lake characteristics. *Freshwater Biology* **52**: 814-822.

Helms JR, Stubbins A, Ritchie JD, Minor EC, Kieber DJ, Mopper K. 2008. Absorption spectral slopes and slope ratios as indicators of molecular weight, source, and photobleaching of chromophoric dissolved organic matter. *Limnology and Oceanography* **53**: 955-969.

Helms JR, Stubbins A, Perdue EM, Green NW, Chen H, Mopper K. 2013. Photochemical bleaching of oceanic dissolved organic matter and its effect on absorption spectral slope and fluorescence. *Marine Chemistry* **115**: 81-91.

Hernes PJ, Bergamaschi BA, Eckard RS, Spencer RGM. 2009. Fluorescence based proxies for lignin in freshwater dissolved organic matter. *Journal Geophysical Research* **114**: G00F03. DOI: 10.1029/2009JG000938.

Hiriart-Baer VP, Diep N, Smith REH. 2008. Dissolved organic matter in the Great Lakes: Role and nature of allochthonous material. *Journal of the Great Lakes Research* **34**: 383-394.

Huguet A, Vacher L, Relexans S, Saubusse S, Froidefond JM, Parlanti E. 2009. Properties of fluorescent dissolved organic matter in the Gironde Estuary. *Organic Geochemistry* **40**: 706-719.

Intergovernmental Panel on Climate Change (IPCC) 2013. Summary for policymakers: Climate change 2013–the physical science basis. In, *Working Group 1 contribution to the IPCC fifth assessment report of the Intergovernmental Panel on Climate Change*, Stocker TF and others (eds). Cambridge University Press: New York; 1-27.

Iriondo M. 1989. Quaternary Lakes of Argentina. *Palaeogeography, Palaeoclimatology, Palaeoecology* **70**: 81-88.

Ishii S, Boyer TH. 2012. Behavior of reoccurring PARAFAC components in fluorescent dissolved organic matter in natural and engineered systems: a critical review. *Environmental Science and Technology* **46**: 2006-2017.

Kalbitz K, Schmerwitz J, Schwesig D, Matzner E. 2003. Biodegradation of soil-derived dissolved organic matter as related to its properties. *Geoderma* **113**: 273– 291.

Kellerman AM, Dittmar T, Kothawala DN, Tranvik LJ. 2014. Chemodiversity of dissolved organic matter in lakes driven by climate and hydrology. *Nature communications* 5: 3804. DOI: 10.1038/ncomms4804

Kellerman AM, Kothawala DN, Dittmar T, Tranvik LJ. 2015. Persistence of dissolved organic matter in lakes related to its molecular characteristics. *Nature Geoscience* **8**: 454–457.

Köhler SJ, Kothawala D, Futter MN, Liungman O, Tranvik L. 2013. In-lake processes offset increased terrestrial inputs of Dissolved Organic Carbon and color to lakes. *PLoS One* **8**: 1-12.

Kothawala DN, Stedmon CA, Müller RA, Weyhenmeyer GA, Kohler SJ, Tranvik LJ. 2014. Controls of dissolved organic matter quality: evidence from a large-scale boreal lake survey. *Global Change Biology* **20**: 1101-1114.

Kowalczuk P, Durako MJ, Young H, Kahn AE , Cooper WJ, Gonsior M. 2009. Characterization of dissolved organic matter fluorescence in the South Atlantic Bight with use of PARAFAC model: Interannual variability. *Marine Chemistry* **113**: 182-196.

Lapierre JF, Guillemette F, Berggren M, del Giorgio PA. 2013. Increases in terrestrially derived carbon stimulate organic carbon processing and CO_2 emissions in boreal aquatic ecosystems. *Nature Communications* **4**: 2972. DOI: 10.1038/ ncomms3972.

Larsen S, Andersen T, Hessen D. 2011. Climate change predicted to cause severe increase of organic carbon in lakes. *Global Change Biology* **17**: 1186-1192. Leps J, Šmilauer T. 2003. *Multivariate analysis of ecological data using CANOCO*, Cambridge University Press, Cambridge.

Lirio JM. 2011. *Eventos paleoambientales en la cuenca del Lago Nahuel Huapi registrados en testigos sedimentarios lacustres durante los últimos 19.000 años*. PhD Thesis. University of Buenos Aires.

Luengen AC, Fisher NS, Bergamaschi BA. 2012. Dissolved organic matter reduces algal accumulation of methylmercury. *Environmental Toxicology and Chemistry* **31**: 1712-1719.

Maie N, Scully NM, Pisani O, Jaffé R. 2007. Composition of a protein-like fluorophore of dissolved organic matter in coastal wetland and estuarine ecosystems. *Water Research* **41**: 563-570.

Masiokas MH, Villalba R, Luckman BH, Lascano ME, Delgado S, Stepanek P. 2008. 20th-Century glacier recession and regional hydroclimatic changes in North-Western Patagonia. *Global and Planetary Change* **60**: 85-100.

Massicotte P, Frenette JJ. 2011. Spatial connectivity in a large river system: resolving the sources and fate of dissolved organic matter. *Ecological Applications* **21**: 2600-2617.

Mcknight D, Boyer E, Westerhoff P, Doran P, Kulbe T, Andersen DT. 2001. Spectrofluorometric characterization of dissolved organic matter for indication of precursor organic material and aromaticity. *Limnology and Oceanography* **46 (1)**: 38-48

Monteith DT, Stoddard JL, Evans CD, de Wit HA, Forsius M, Høgasen T, Wilander A, Skjelkva Vuorenmaa J, Keller B, Kopale BL, Jeffries DS, Kopacek J, Vesely J. 2007. Dissolved organic carbon trends resulting from changes in atmospheric deposition chemistry. *Nature* **450**: 537-541.

Moran MA, Sheldon Jr WM, Zepp RG. 2000. Carbon loss and optical property changes during long-term photochemical and biological degradation of estuarine dissolved organic matter. *Limnology and Oceanography* **45**: 1254-1264.

Morris DP, Zagarese HE, Williamson CE, Balseiro EG, Hargreaves BR, Modenutti BE, Moeller R, Queimaliños C. 1995. The attenuation of UV radiation in lakes and the role of dissolved organic carbon. *Limnology and Oceanography* **40**: 1381-91.

Murphy KR, Butler K, Spencer RM, Stedmon CA, Boehme J, Aiken GR. 2010. Measurement of dissolved organic matter fluorescence in aquatic environments: an interlaboratory comparison. *Environmental Science and Technology* **44**: 9405-9412.

Murphy KR, Stedmon CA, Graeber D, Bro R. 2013. Fluorescence spectroscopy and multi-way techniques. PARAFAC. *Analytical Methods* **5**: 6557-6566.

Murphy KR, Stedmon CA, Wenig P, Bro R. 2014. OpenFluor – an online spectral library of auto-fluorescence by organic compounds in the environment. *Analytical Methods* **6**: 658–661.

Nõges T. 2009. Relationships between morphometry, geographic location and water quality parameters of European lakes. *Hydrobiologia* **633**: 33-43.

Nusch EA. 1980. Comparison of different methods for chlorophyll and pheopigment determination. *Archiv für Hydrobiologie* **14**: 14-36.

Ohno T. 2002. Fluorescence inner-filtering correction for determining the humification index of dissolved organic matter. *Environmental Science and Technology* **36**: 742-746.

Pace MJ, Cole CC. 2002. Synchronous variation of dissolved organic carbon and color in lakes. *Limnology and Oceanography* **47(2)**: 333-342.

Paruelo JM, Beltran A, Jobbagy E, Sala OE, Golluscio RA. 1998. The climate of Patagonia: general patterns and controls on biotic processes. *Ecología Austral* **8(2)**: 85-101.

Perakis SS, Hedin LO. 2002. Nitrogen loss from unpolluted South American forests mainly via dissolved organic compounds. *Nature* **415**: 416-419.

Pérez GL, Torremorell A, Bustingorry J, Escaray R, Pérez P, Diéguez M, Zagarese H. 2010. Optical characteristics of shallow lakes from the Pampa and Patagonia regions of Argentina. *Limnologica* **40:** 30-39.

Queimaliños CP, Reissig M, Diéguez MC, Arcagni M, Ribeiro Guevara S, Campbell L, Soto Cárdenas C, Rapacioli R, Arribére M. 2012. Influence of precipitation, landscape and hydrogeomorphic lake features on pelagic allochthonous indicators in two connected ultraoligotrophic lakes of North Patagonia. *Science of the Total Environment* **427-428**: 219-228.

Queimaliños C. 2002. The role of phytoplanktonic size fractions in the microbial food webs in two north Patagonian lakes (Argentina). Verhandlungen des Internationalen Verein Limnologie 28: 1236–1240.

Rapacioli RA. 2011. Caracterización hidrológica de la Reserva Natural Urbana Lago Morenito – Laguna Ezquerra. In *Proyecto de Manejo de Reserva Natural Morenito-Ezquerra.* Abalerón A (ed), Fundación Bariloche: Bariloche; 1-38.

Ravichandran M. 2004. Interactions between mercury and dissolved organic matter – a review. *Chemosphere* **55**: 319-31.

Read JS, Rose KC. 2013. Physical responses of small temperate lakes to variation in dissolved organic carbon concentrations. *Limnology and Oceanography* **58**: 921-931.

Reche I. 2003. Sensibilidad de los ecosistemas acuáticos a la radiación ultravioleta: el papel de la materia orgánica disuelta. *Ecosystems* **12:** 1-11.

Reche I, Pace ML, Cole JJ. 1999. Relationship of trophic and chemical conditions to photobleaching of dissolved organic matter in lake ecosystems. *Biogeochemistry* **44**: 259-280.

Reche I, Pace ML, Cole JJ. 2000. Modeled effects of dissolved organic carbon and solar spectra on photobleaching in lake ecosystems. *Ecosystems* **3**: 419-432.

Ribeiro Guevara S, Queimaliños CP, Diéguez MC, Arribére M. 2008. Methylmercury production in the water column of an ultraoligotrophic lake of Northern Patagonia, Argentina. *Chemosphere* **72**: 578-585.

Rizzo A, Arcagni M, Arribére MA, Bubach D, Ribeiro Guevara S. 2011. Mercury in the biotic compartments of Northwest Patagonia lakes, Argentina. *Chemosphere* 84: 70–79.

Rizzo A, Arcagni M, Campbell LM, Koron N, Pavlin, M, Arribére MA, Horvat M, Ribeiro Guevara S. 2014. Source and trophic transfer of mercury in plankton from an ultraoligotrophic lacustrine system (Lake Nahuel Huapi, North Patagonia). *Ecotoxicology* 23(7): 1184–1194.

Roulet N, Moore TR. 2006. Browning the waters. *Nature* **444**: 283-284.

Shutova Y, Baker A, Bridgeman J, Henderson RK. 2014. Spectroscopic characterization of dissolved organic matter changes in drinking water treatment: From PARAFAC analysis to online monitoring wavelengths. *Water Research* **54**: 159-169.

Sommaruga R, Augustin G. 2006. Seasonality in UV transparency of an alpine lake is associated to changes in phytoplankton biomass. *Aquatic Sciences* **68**: 129-141.

Soto Cárdenas C, Diéguez MC, Ribeiro Guevara S, Marvin-DiPasquale M, Queimaliños. CP. 2014. Incorporation of inorganic mercury (Hg^{2+}) in pelagic food webs of ultraoligotrophic and oligotrophic lakes: the role of different plankton size fractions and species assemblages. *Science of the Total Environment* **494–495**: 65–73

Soto Cárdenas C. 2015. Caracterización de la Materia Orgánica Disuelta y su relación con el Mercurio en lagos Norpatagónicos. Ph.D Thesis. Universidad Nacional del Comahue, Argentina.

Spencer RGM, Aiken GR, Butler KD, Dornblaser MM, Striegl RG, Hernes PJ. 2009. Utilizing chromophoric dissolved organic matter measurements to derive export and reactivity of dissolved organic carbon exported to the Arctic Ocean: a case study of the Yukon River, Alaska. *Geophysical Research Letters* **36**: L06401.

Stedmon CA, Markager S. 2005. Resolving the variability in dissolved organic matter fluorescence in a temperate estuary and its catchment using PARAFAC analysis. *Limnology and Oceanography* **50**: 686-697.

Stedmon CA, Markager S, Bro R. 2003. Tracing dissolved organic matter in aquatic environments using a new approach to fluorescence spectroscopy. *Marine Chemistry* **82**: 239-254.

Stubbins A, Lapierre JF, Berggren M, Prairie YT, Dittmar T, del Giorgio PA. 2014. What's in an EEM? Molecular signatures associated with dissolved organic fluorescence in boreal Canada. *Environmental Science and Technology* **48**: 10598-10606.

Stubbins A, Spencer RGM, Chen H, Hatcher PG, Mopper K, Hernes PJ, Mwamba VL, Mangangu AM, Wabakanghanzi JN, Six J. 2010. Illuminated darkness: Molecular signatures of Congo River dissolved organic matter and its photochemical alteration as revealed by ultrahigh precision mass spectrometry. *Limnology and Oceanography* **55**: 1467-1477.

ter Braak CJF, Šmilauer P. 1998. *CANOCO reference manual and user's guide to Canoco for Windows – software for canonical community ordination (version 4)*. Microcomputer Power, Ithaca, NY.

Thrane JE, Hessen DO, Andersen T. 2014. The absorption of light in lakes: negative impact of dissolved organic carbon on primary productivity. *Ecosystems* **17**: 1040-1052.

Twardowsky MS, Donaghay PL. 2001. Separating in situ and terrigenous sources of absorption by dissolved materials in coastal waters. *Journal Geophysical Research* **106**: 2545-2560.

Vogt RJ, Rusak JA, Patoine A, Leavitt PR. 2011. Differential effects of energy and mass influx on the landscape synchrony of lake ecosystems. *Ecology* 92(5): 1104-1114.

Van Gaelen N, Verheyen D, Ronchi B, Struyf E, Govers G, Vanderborght J, Diels J. 2014. Identifying the transport pathways of dissolved organic carbon in contrasting catchments. *Vadose Zone Journal* **13(7)**. doi:10.2136/vzj2013.11.0199

von Wachenfeldt E, Sobek S, Bastviken D, Tranvik LJ. 2008. Linking allochthonous dissolved organic matter and boreal lake sediment carbon sequestration: The role of light- mediated flocculation. *Limnology and Oceanography* **53**: 2416-2426.

Webster KE, Soranno PA, Cheruvelil KS, Bremigan MT, Downing JA, Vaux PD, Asplund TR, Bacon LC, Connor J. 2008. An empirical evaluation of the nutrient– color paradigm for lakes. *Limnology and Oceanography* **53:** 1137-1148.

Wei J, Han L, Song J, Chen M. 2015. Evaluation of the interactions between water extractable soil organic matter and metal cations (Cu(II), Eu(III)) using Excitation-Emission Matrix combined with Parallel Factor Analysis. *International Journal of Molecular Sciences* **16**: 14464-14476.

Weishaar JL, Aiken GR, Bergamaschi BA, Fram MS, Fujii R, Mopper K. 2003. Evaluation of specific ultraviolet absorbance as an indicator of the chemical composition and reactivity of dissolved organic carbon. *Environmental Science and Technology* **37**: 4702-4708.

Wetzel RG. 2001. Limnology: Lake and River Ecosystems. San Francisco: Academic Press.

Weyhenmeyer GA, Karlsson J. 2009. Nonlinear response of dissolved organic carbon concentrations in boreal lakes to increasing temperatures. *Limnology and Oceanography* **54:** 2513-2519.

Weyhenmeyer GA, Müller RA, Norman M, Tranvik LJ. 2016. Sensitivity of freshwaters to browning in response to future climate change. *Climatic Change*, **134**: 225-239. Williamson CE, Brentrup JA, Zhang J, Renwick WH, Hargreaves BR, Knoll LB, Overholt EP, Rose KC. 2014. Lakes as sensors in the landscape: optical metrics as scalable sentinel responses to climate change. *Limnology and Oceanography* **59:** 840-850.

Yamashita Y, Kloeppel BD, Knoepp J, Zausen GL, Jaffé R. 2011. Effects of watershed history on dissolved organic matter characteristics in headwater streams. *Ecosystems* **14**: 1110-1122.

Yamashita Y, Cory RM, Nishioka J, Kuma K, Tanoue E, Jaffé R. 2010. Fluorescence characteristics of dissolved organic matter in the deep waters of the Okhotsk Sea and the northwestern North Pacific Ocean. *Deep-Sea Research Part II* **57**: 1478-1485.

Zagarese HE, Tartarotti B, Cravero W, Gonzalez P. 1998. UV damage in shallow lakes: the implications of water mixing. *Journal of Plankton Research* **20**: 1423-1433.

Zagarese HE, Diaz M, Pedrozo F, Ferraro M, Cravero W, Tartarotti B. 2001. Photodegradation of natural organic matter exposed to fluctuating levels of solar radiation. *Journal of Photochemistry and Photobiology B: Biology* **61**: 35–45.

Zhang Y, van Dijk MA, Liu M, Zhua G, Qin B. 2009. The contribution of phytoplankton degradation to chromophoric dissolved organic matter (CDOM) in eutrophic shallow lakes: Field and experimental evidence. *Water Research* **43**: 4685-4697.

Zhang Y, Zhang E, Yin Y, van Dijk MA, Feng L, Shi Z, Liu M, Qin B. 2010. Characteristics and sources of chromophoric dissolved organic matter in lakes of the Yungui Plateau, China, differing in trophic state and altitude. *Limnology and Oceanography* **55:** 2645-2659.

Zhou Y, Zhang Y, Shi K, Liu X, Niu C. 2015. Dynamics of chromophoric dissolved organic matter influenced by hydrological conditions in a large, shallow, and eutrophic lake in China. *Environmental Science Pollution Research* **22(17)**: 12992–13003

Zsolnay Á, Baigar E, Jimenez M, Steinweg B, Saccomandi F. 1999. Differentiating with fluorescence spectroscopy the sources of dissolved organic matter in soils subjected to drying. *Chemosphere* **38**: 45–50.

Figure Captions

Figure 1. A) Location of the shallow lakes Morenito and Escondido inside Nahuel Huapi basin (North Patagonia, Argentina); B) Drainage catchments of lakes Morenito and Escondido and connection between lakes Morenito, Moreno West and Ezquerra; C) Satellite images of lakes Morenito and Escondido obtained during the low water phase (dry season). Floodplain areas during the high water phase (wet season) are delimited with dotted lines in B and indicated with white arrows in C and D (Google Earth®). Drainage catchments are shown with an orange line in B, C and D. The asterisk in B and D indicates a small, closed water body.

Figure 2. A) Monthly precipitation (gray bars), air temperature (continuous line) and monthly fluence of photosynthetically active radiation (dotted line) at ground level during the three years studied; B) Cumulative precipitation during the 150 days previous to sampling (dark gray bars) and water storage of Lake Nahuel Huapi (dashed line), depicting the fluctuation of water level in the basin from 2013 to 2015. Arrows indicate sampling dates.

Figure 3. Box plots showing the fluctuation of: A) dissolved organic carbon (DOC) concentration and B) whole lake DOC mass, in Lake Morenito and Lake Escondido during the wet (gray panel) and dry (yellow panel) seasons for the three years studied. Whiskers indicate the minimum and maximum values, lower and upper ends of boxes indicate lower and upper quartiles, the solid line indicates the median, and the dashed line indicates the average. Circles indicate outliers above and below the 95^{th} and 5^{th} percentiles.

Figure 4. Box plots showing the fluctuation of absorption coefficient a_{350} (proxy of CDOM) in Lake Morenito and Lake Escondido during the wet (gray panel) and the dry (yellow panel) seasons in the three years studied. Whiskers indicate the minimum and maximum values, lower and upper ends of boxes indicate lower and upper quartiles, the solid line indicates the median, and the dashed line indicates the average. Circles indicate outliers above and below the 95^{th} and 5^{th} percentiles.

Figure 5. Relationship between: A) the DOC normalized absorption coefficient at 350 nm (a_{350}:DOC) and the spectral slope $S_{275–295}$; B) the humification index (HIX) and the index of recent biologically produced DOM (BIX) in Lake Morenito (triangles) and Lake Escondido (circles). Data are presented as means ± standard deviation. The arrows inside the main figure A) indicate the pattern and directions of change due to photochemical transformation along the gradients of water residence time (WRT) and terrestrial fresh DOM inputs, within an explanatory model (Fichot and Benner, 2012; Anderson and Stedmon, 2007; Williamson *et al.*, 2014). The color scale represents cumulative precipitation.

Figure 6. Left panel: box plots showing the fluorescence intensity (in Raman Units, R.U.) of the FDOM components (A: C1; B: C2, and C: C3) in the wet (gray panel) and the dry (yellow panel) seasons in lakes Morenito and Escondido. Black circles represent outliers beyond the 95^{th} and 5^{th} percentiles. Right panel: relationship between the fluorescent components as percentage and the $S_{275-295}$ in lakes Morenito and Escondido (D: % C1; E: % C2 and F: % C3). The arrows inside the main figure E) indicate the pattern and directions of change due to photochemical transformation along the gradients of water residence time (WRT) and terrestrial fresh DOM inputs, within an explanatory model. These arrows also imply figure D and F.

Figure 7. Redundancy analysis (RDA) including all water samples (n=44). DOM parameters as response variables: DOC, a_{350}:DOC, $S_{275-295}$, BIX, HIX, the intensity of components C1, C2 and C3 are indicated by blue arrows. Significant environmental variables ($p< 0.05$): cumulative precipitation (Prec 150 days), perimeter:area ratio (P:A), fluence (fluence 150 days), % Water, Chl*a* and water temperature (W-Temp) are indicated by red arrows.

Supporting Figure S1. Profiles of lakes Morenito and Escondido comparing lake area and volume in the wet and dry seasons.

Table 1. Geographic location and hydrogeomorphic features of lakes Morenito and Escondido detailed for the dry and wet seasons when applicable. Abbreviations are as follows: Q_{mv}, mean annual (or seasonal) water discharge; WRT, water retention time. * % Water was calculated only considering the upstream contribution of Laguna Ezquerra to Lake Morenito.

	Lake Morenito		**Lake Escondido**	
Geographic location	41°03´S 71°31´ W		41°03´S 71°34´ W	
Hydrogeomorphic features	Wet season	Dry season	Wet season	Dry season
Lake area (A) (km^2)	0.364	0.294	0.095	0.086
Maximum depth (Zmax) (m)	10.5	8.5	8.3	7.8
Lake Volume (V) (hm^3)	1.87	1.23	0.50	0.44
% increase in water volume between seasons	52.13		12.95	
Mean depth (Z_{mean}) (m)	5.2	5.0	5.2	5.1
Lake perimeter (km)	4.43	3.53	1.59	1.33
Lake perimeter:lake area ratio (km^{-1})	12.17	12.01	16.74	15.46
Seasonal Q_{mv} (L s^{-1})	199.67	1.25	50.59	2.52
Annual Q_{mv} (L s^{-1})	70.54		26.3	
WRT (years)	0.50		0.56	
Catchment features				
Drainage area (D) (km^2)	1.495		0.419	
Drainage ratio (D:A)	4.16	6.10	4.41	4.87
% Water*	7.63	3.57	0	0
% Forest	91		100	
% Urban area	9		0	

Table 2. Mean values (± 1 SD) of dissolved organic carbon (DOC) concentration, DOC mass, a_{350}, colored DOM (a_{440}), aromaticity ($SUVA_{254}$), a_{350}:DOC, spectral slope between 275 and 295 nm ($S_{275-295}$); biological index (BIX), humification index (HIX), PARAFAC components C1, C2 and C3, normalized by DOC components (Ci:DOC), and percentage components in the dry and wet seasons. Significant differences are indicated with asterisks (*p<0.001). Homogeneous groups (a, b, c and d) were tested with Bonferroni *t*-test (p<0.001).

	Lake Morenito		Lake Escondido		One-way ANOVA	Bonferroni *t*-test			
						Lake Morenito		Lake Escondido	
	Wet	Dry	Wet	Dry		Wet	Dry	Wet	Dry
Dissolved Organic Carbon Concentration **(mg L^{-1})**									
DOC	2.8 ± 0.2	3.1 ± 0.1	4.0 ± 0.1	3.7 ± 0.3	F = 87.61*	a	b	c	d
Dissolved Organic Carbon Masses **(Ton C $lake^{-1}$)**									
DOC	5.33 ± 0.39	3.80 ± 0.14	2.01 ± 0.07	1.64 ± 0.11	F = 1185.96*	a	b	c	d
CDOM features									
a_{350} **(m^{-1})**	3.17 ± 0.28	1.86 ± 0.06	6.73 ± 0.36	3.34 ± 0.14	F = 896.01*	a	b	c	a
a_{440} **(m^{-1})**	0.67 ± 0.01	0.40 ± 0.04	1.40 ± 0.10	0.63 ± 0.03	F = 383.74*	a	b	c	a
$SUVA_{254}$	3.13 ± 1.27	1.70 ± 0.08	3.02 ± 0.21	2.16 ± 0.12	F = 155.0*	a	b	c	a
a_{350}**: DOC**	1.12 ± 0.13	0.60 ± 0.02	1.68 ± 0.10	0.91 ± 0.06	F = 249.63*	a	b	c	d
$S_{275-295}$ **(10^{-3} nm^{-1})**	18.90 ± 1.00	24.6 ± 0.20	16.90 ± 0.60	21.8 ± 0.40	F = 339.4*	a	b	c	d
FDOM features									
BIX	0.58 ± 0.04	0.73 ± 0.02	0.51 ± 0.02	0.63 ± 0.03	F = 155.99*	a	b	c	d
HIX	0.89 ± 0.03	0.85 ± 0.02	0.92 ± 0.003	0.89 ± 0.02	F = 23.69*	a	b	c	a
C1 (R.U.)	0.33 ± 0.03	0.29 ± 0.02	0.54 ± 0.05	0.44 ± 0.03	F =146.41 *	a	b	c	d
C2 (R.U.)	0.21 ± 0.04	0.13 ± 0.02	0.36 ± 0.04	0.21 ± 0.03	F = 93.41*	a	b	c	a
C3 (R.U.)	0.09 ± 0.01	0.11 ± 0.007	0.08 ± 0.01	0.11 ± 0.01	F =11.94*	a	b	a	b
%C1	52.6 ± 3.1	55.4 ± 1.7	54.7 ± 3.1	58.2 ± 1.5	F = 41.74 *	a	b	ab	c
%C2	32.5 ± 3.6	24.1 ± 2.5	36.6 ± 2.5	27.6 ± 2.8	F = 11.59*	a	b	c	d
%C3	14.9 ± 1.6	20.5 ± 2.1	8.6 ± 1.5	14.3 ± 1.5	F = 92.09*	a	b	c	a

Table 3. Fluorescence peak locations [Excitation/Emission (Ex/Em), secondary peak in parentheses], representative excitation-emission matrices (EEMs) and spectral loadings of the three components identified by the PARAFAC model. The components are shown in decreasing order of emission values (nm). References: Trad. Class.: traditional classification.

Component	Ex/Em maximum	EEM	Loading	Trad. class.	Other study matches*	Visible spectra**	Persistence in landscape [1*]
C2	240 (345)/ 460	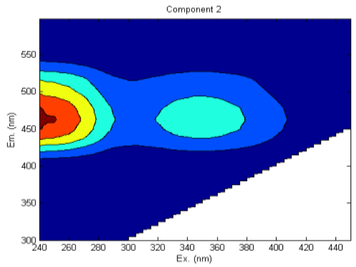	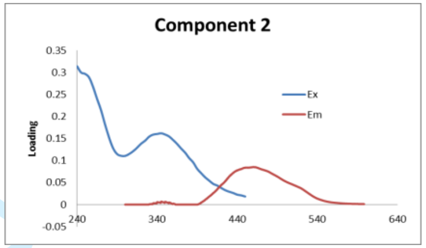	A+C	C1: Shutova *et al.*, 2014 C1: Yamashita *et al.*, 2010	high color high aromaticity	high reactivity high susceptibility to photobleaching and flocculation
C1	240 (305)/ 396	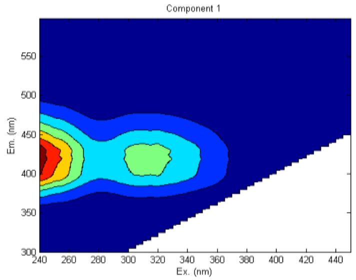	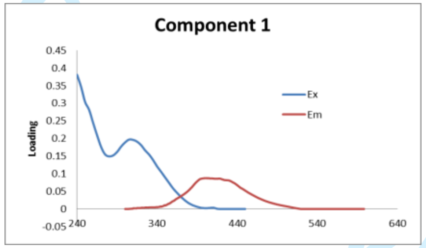	A+M	C1: Cawley *et al.*, 2012 C1: Graeber *et al.*, 2012	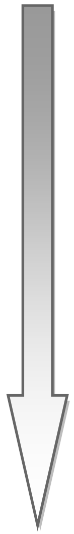	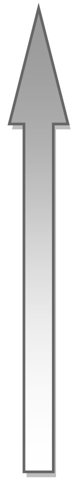
C3	240 (280)/ 361.5	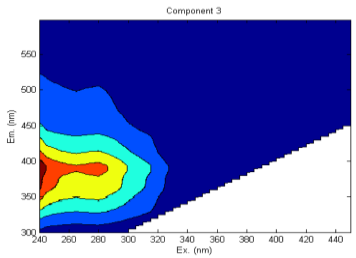	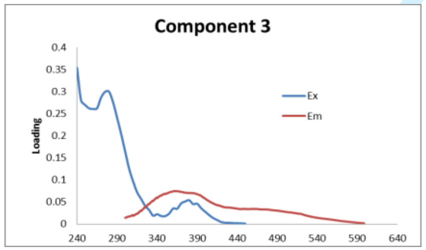	T	C3: García *et al.*, 2015	less color low aromaticity	low reactivity high persistence

* Similarities of our components to previous fluorescence spectra included in the open-access database OpenFluor (www.openfluor.org, Murphy *et al.*, 2014),
** The diagrams shown on the right hand margin have been modified from Kothawala *et al.* (2014).

Supporting Table 1. Pearson correlation between optical variables and DOC-normalized FDOM components with cumulative rain 150 days before sampling (n=44). Significant values in bold.

Variable	r	p value
a_{350}:DOC - precipitation	0.74	*<0.001*
a_{440} - precipitation	0.60	*<0.001*
$S_{275\text{-}295}$ - precipitation	-0.85	*<0.001*
BIX - precipitation	-0.67	*<0.001*
HIX - precipitation	0.49	*<0.001*
C1 -precipitation	0.25	*0.09*
C2 -precipitation	0.49	*<0.001*
C3 -precipitation	-0.52	*<0.001*
%C1 -precipitation	-0.38	*0.01*
%C2 -precipitation	0.61	*<0.001*
%C3 -precipitation	-0.50	*<0.001*

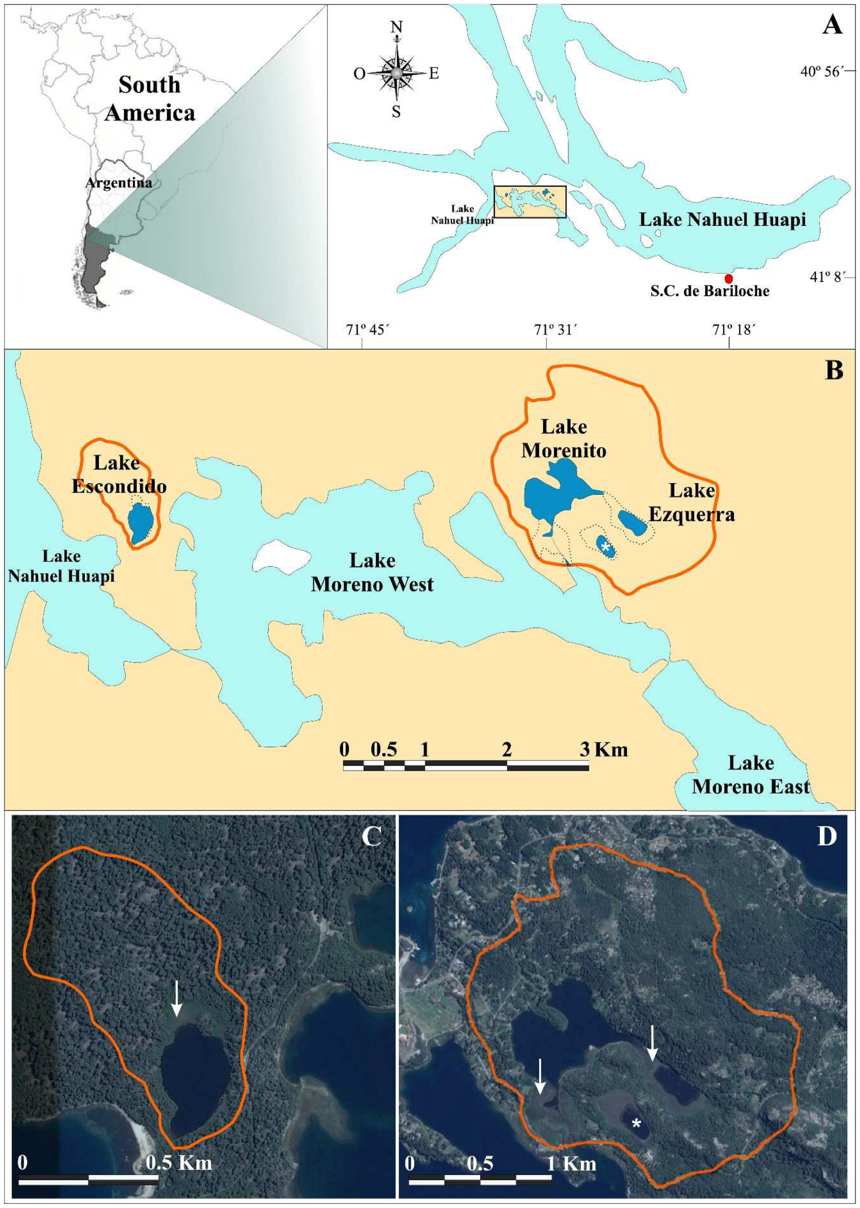

Figure 1. A) Location of the shallow lakes Morenito and Escondido inside Nahuel Huapi basin (North Patagonia, Argentina); B) Drainage catchments of lakes Morenito and Escondido and connection between lakes Morenito, Moreno West and Ezquerra; C) Satellite images of lakes Morenito and Escondido obtained during the low water phase (dry season). Floodplain areas during the high water phase (wet season) are delimited with dotted lines in B and indicated with white arrows in C and D (Google Earth®). Drainage catchments are shown with an orange line in B, C and D. The asterisk in B and D indicates a small, closed water body.

457x643mm (600 x 600 DPI)

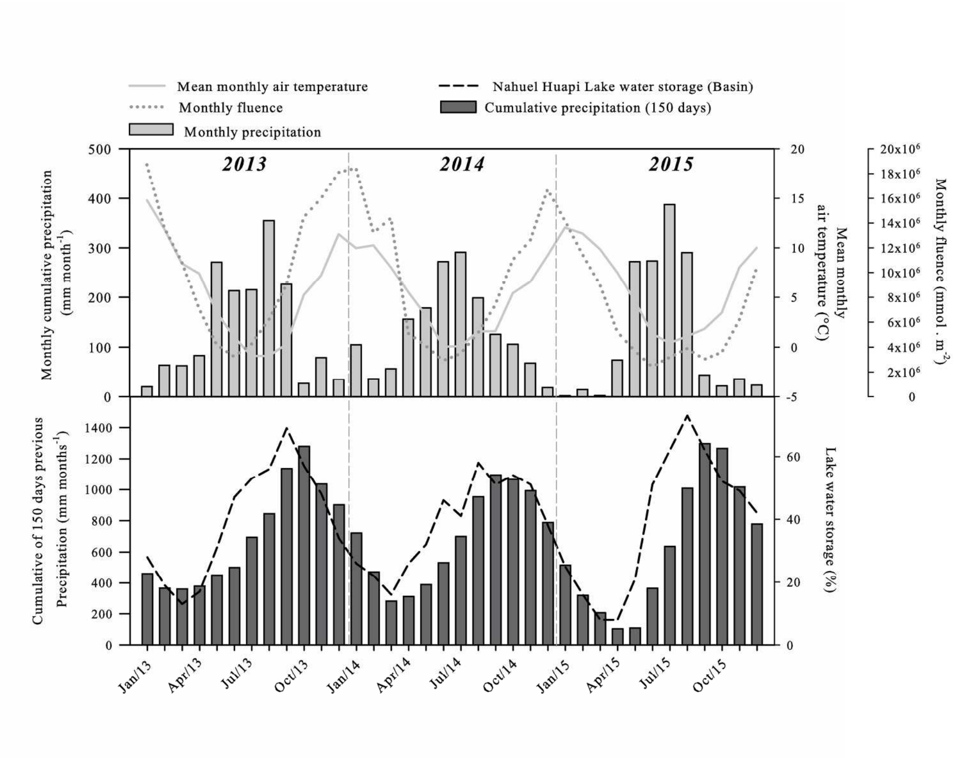

Figure 2. A) Monthly precipitation (gray bars), air temperature (continuous line) and monthly fluence of photosynthetically active radiation (dotted line) at ground level during the three years studied; B) Cumulative precipitation during the 150 days previous to sampling (dark gray bars) and water storage of Lake Nahuel Huapi (dashed line), depicting the fluctuation of water level in the basin from 2013 to 2015. Arrows indicate sampling dates.

194x152mm (300 x 300 DPI)

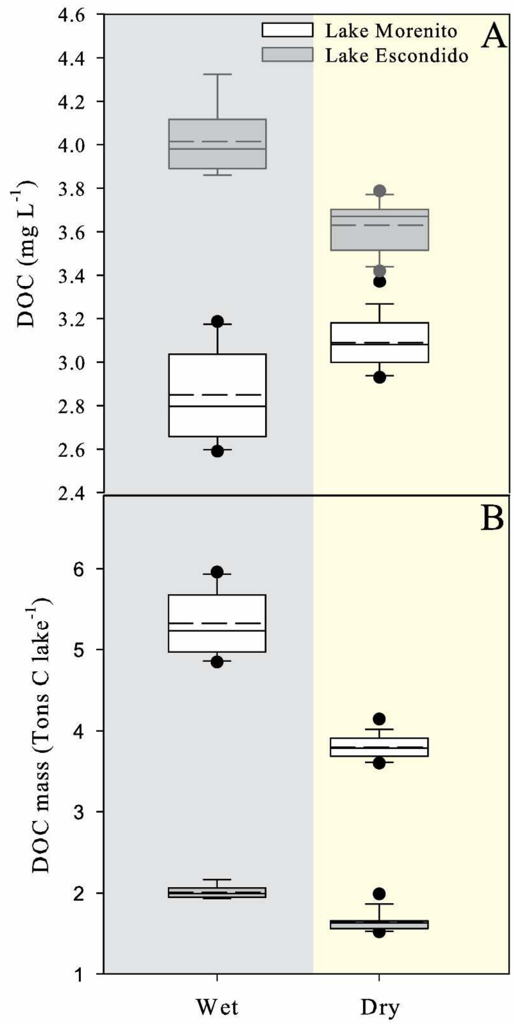

Figure 3. Box plots showing the fluctuation of: A) dissolved organic carbon (DOC) concentration and B) whole lake DOC mass, in Lake Morenito and Lake Escondido during the wet (gray panel) and dry (yellow panel) seasons for the three years studied. Whiskers indicate the minimum and maximum values, lower and upper ends of boxes indicate lower and upper quartiles, the solid line indicates the median, and the dashed line indicates the average. Circles indicate outliers above and below the 95th and 5th percentiles.

225x462mm (300 x 300 DPI)

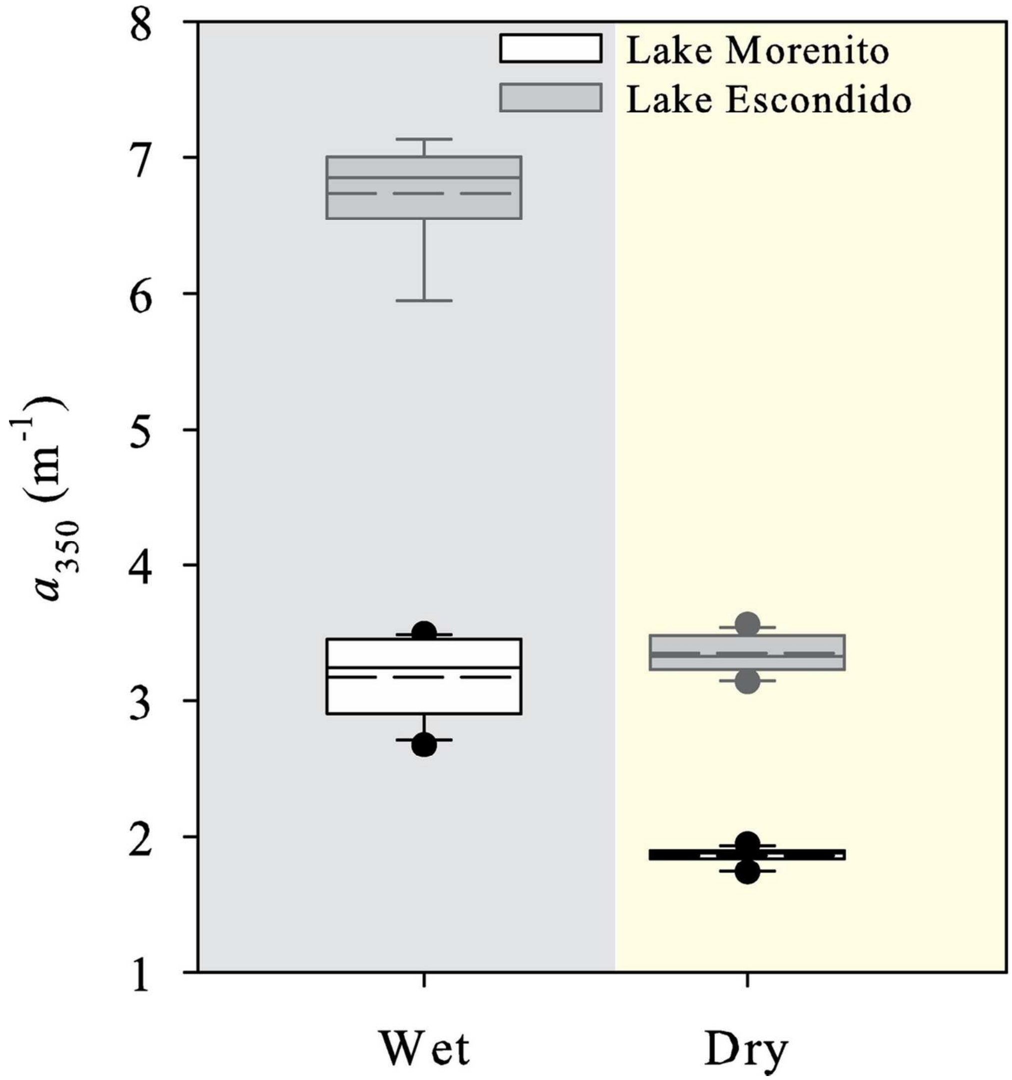

Figure 4. Box plots showing the fluctuation of absorption coefficient a_{350} (proxy of CDOM) in Lake Morenito and Lake Escondido during the wet (gray panel) and the dry (yellow panel) seasons in the three years studied. Whiskers indicate the minimum and maximum values, lower and upper ends of boxes indicate lower and upper quartiles, the solid line indicates the median, and the dashed line indicates the average. Circles indicate outliers above and below the 95th and 5th percentiles.

101x108mm (300 x 300 DPI)

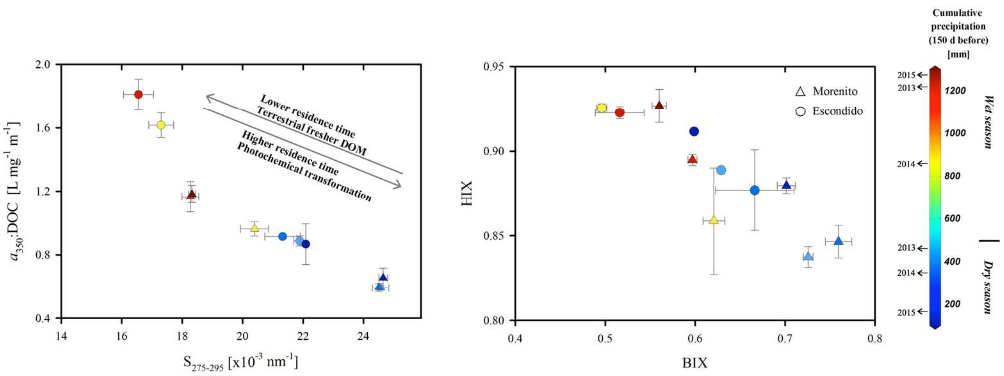

Figure 5. Relationship between: A) the DOC normalized absorption coefficient at 350 nm (a_{350}:DOC) and the spectral slope $S_{275–295}$; B) the humification index (HIX) and the index of recent biologically produced DOM (BIX) in Lake Morenito (triangles) and Lake Escondido (circles). Data are presented as means ± standard deviation. The arrows inside the main figure A) indicate the pattern and directions of change due to photochemical transformation along the gradients of water residence time (WRT) and terrestrial fresh DOM inputs, within an explanatory model (Fichot and Benner, 2012; Anderson and Stedmon, 2007; Williamson et al., 2014). The color scale represents cumulative precipitation.

158x71mm (300 x 300 DPI)

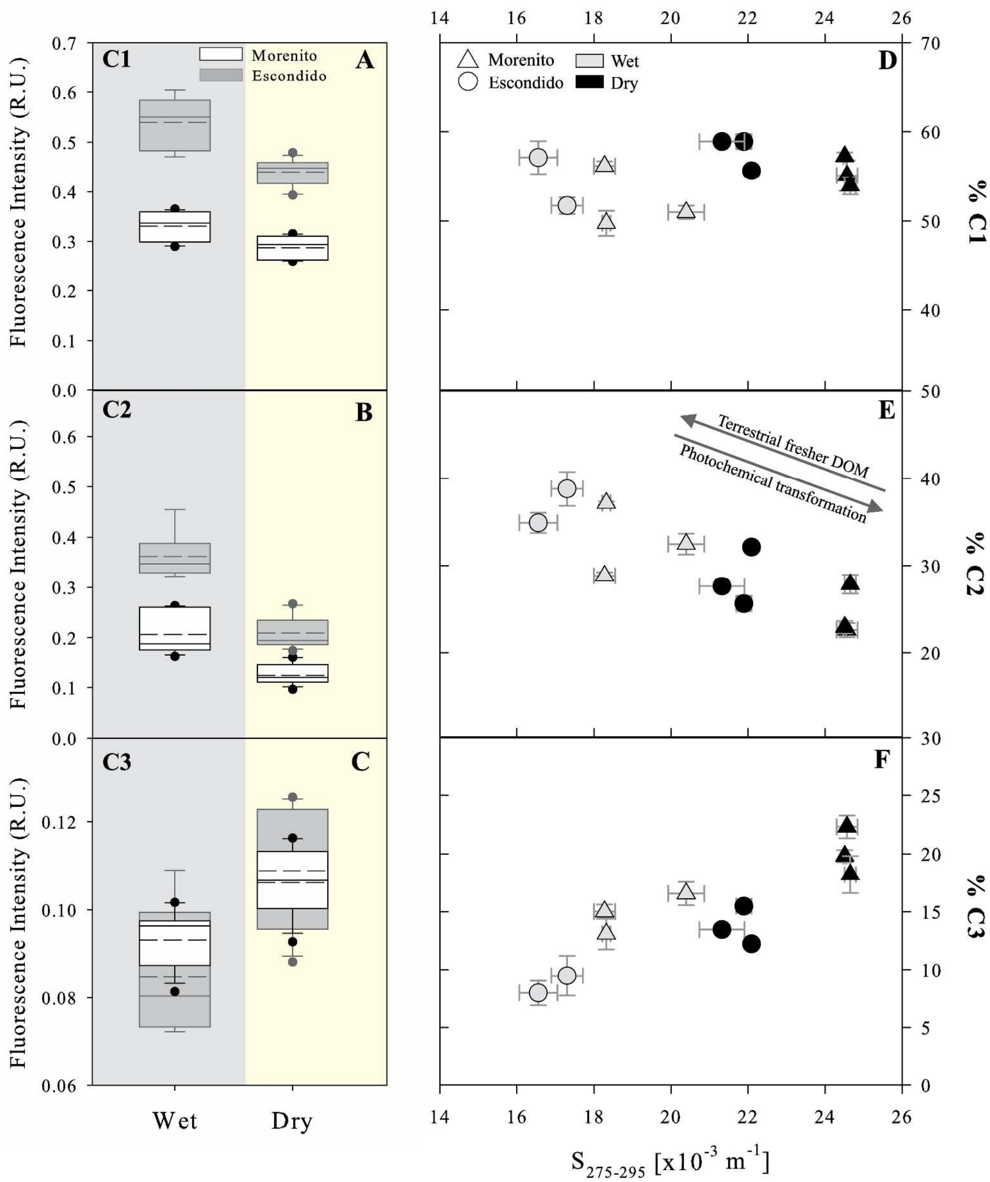

Figure 6. Left panel: box plots showing the fluorescence intensity (in Raman Units, R.U.) of the FDOM components (A: C1; B: C2, and C: C3) in the wet (gray panel) and the dry (yellow panel) seasons in lakes Morenito and Escondido. Black circles represent outliers beyond the 95th and 5th percentiles. Right panel: relationship between the fluorescent components as percentage and the $S_{275-295}$ in lakes Morenito and Escondido (D: % C1; E: % C2 and F: % C3). The arrows inside the main figure E) indicate the pattern and directions of change due to photochemical transformation along the gradients of water residence time (WRT) and terrestrial fresh DOM inputs, within an explanatory model. These arrows also imply figure D and F.

310x378mm (300 x 300 DPI)

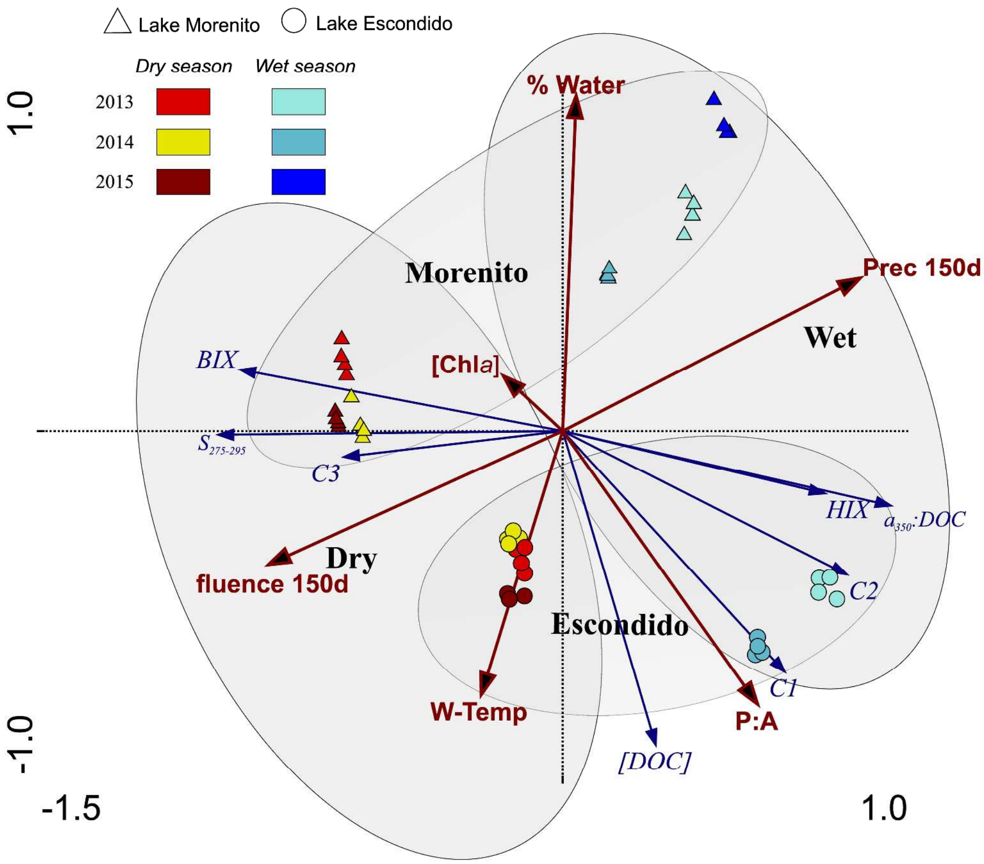

Figure 7. Redundancy analysis (RDA) including all water samples (n=44). DOM parameters as response variables: DOC, a_{350}:DOC, $S_{275\text{-}295}$, BIX, HIX, the intensity of components C1, C2 and C3 are indicated by blue arrows. Significant environmental variables ($p < 0.05$): cumulative precipitation (Prec 150 days), perimeter:area ratio (P:A), fluence (fluence 150 days), % Water, Chl*a* and water temperature (W-Temp) are indicated by red arrows.

343x307mm (300 x 300 DPI)

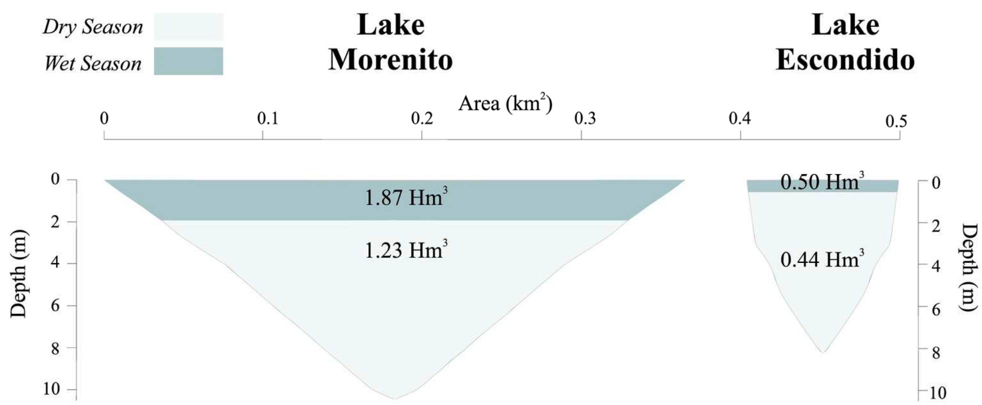

Supporting Figure S1. Profiles of lakes Morenito and Escondido comparing lake area and volume in the wet and dry seasons.

174x77mm (300 x 300 DPI)